Aus der Klinik für Kardiologie, Nephrologie und Pneumologie des Universitätsklinikums
Brandenburg an der Havel und
der Fakultät für Gesundheitswissenschaften Brandenburg
der Medizinischen Hochschule Brandenburg Theodor Fontane

DISSERTATION

NOS1AP alters the QT Interval upon Overexpression in Mice

zur Erlangung des akademischen Grades

Dr. rer. medic. (Doctor rerum medicinalium)

vorgelegt der Fakultät für Gesundheitswissenschaften

Brandenburg

von

Monique Heidrun Jänsch

Datum: 14.07.2023

Zitationsvorschlag:

Jänsch, Monique Heidrun (2023): NOS1AP alters the QT Interval upon Overexpression in Mice. Brandenburg: Medizinische Hochschule Brandenburg Theodor Fontane
DOI: 10.4126/FRL01-006525147

Online veröffentlicht auf dem Fachrepositorium Lebenswissenschaften PUBLISSO:
https://repository.publisso.de/resource

DOI: https://doi.org/10.4126/FRL01-006525147

LIVIVO: https://www.livivo.de/app?LANGUAGE=de

Table of Contents

Author contributions

Publications	Impact Factor	Counts	
		First	Co-
2018			
1. Olivares-Florez S, Czolbe M, Riediger F, Seidlmayer L, Williams T, Nordbeck P, Strasen J, Glocker C, **Jänsch M**, Eder-Negrin P, Arias-Loza P, Mühlfelder M, Plačkić J, Heinze KG, Molkentin JD, Engelhardt S, Kockskämper J, Ritter O. Nuclear calcineurin is a sensor for detecting Ca2+ release from the nuclear envelope via IP3R. *J Mol Med (Berl).* 2018 Nov;96(11):1239-1249.	4.8		1
2021			
2. Sasko B, Patschan D, Nordbeck P, Seidlmayer L, Andresen H, **Jänsch M**, Bramlage P, Ritter O, Pagonas N. Secondary Prevention of Potentially Life-Threatening Arrhythmia Using Implantable Cardioverter Defibrillators in Patients with Biopsy-Proven Viral Myocarditis and Preserved Ejection Fraction. *Cardiology*. 2021;146(2):213-221.	2.7		2
2022			
3. Wang C, Enssle J, Pietzner A, Schmöcker C, Weiland L, Ritter O, **Jaensch M**, Elbelt U, Pagonas N, Weylandt KH. Essential Polyunsaturated Fatty Acids in Blood from Patients with and without Catheter-Proven Coronary Artery Disease. *Int J Mol Sci.* 2022 Jan 11;23(2):766.	5.5		3
4. Lubomirov LT, **Jänsch MH**, Papadopoulos S, Schroeter MM, Metzler D, Bust M, Hescheler J, Grisk O, Ritter O, Pfitzer G. Senescent murine femoral arteries undergo vascular remodelling associated with accelerated stress-induced contractility and reactivity to nitric oxide. *Basic Clin Pharmacol Toxicol.* 2022 Jan;130(1):70-83.	4.1	1	
5. Patschan D, Marahrens B, **Jansch M**, Patschan S, Ritter O. Experimental Cardiorenal Syndrome Type 3: What Is Known so Far? *J Clin Med Res*. 2022 Jan;14(1):22-27.	1		4
Sum of First / Co-Authorship		**1**	**4**

Grants

Rudi-Busse-Young Investigator Award für experimentelle Herz- und Kreislaufforschung
Title: *„Investigations regarding the role of NOS1AP in the heart using a conditional over-expression mouse model“*
Date of oral defense: April, 17th 2020 - 86. Jahrestagung der Deutschen Gesellschaft für Kardiologie (DGK)

Abstracts

85. Jahrestagung der DGK. Mannheim 2019. Posterpräsentation: Nos1ap alters QT intervals upon overexpression in mice. **Jänsch M**, Glocker C, Williams T, Oppelt D, Arias-Loza AP, Schmitt J, Schuh K, Ritter O
88. Jahrestagung der DGK. Mannheim 2022. Posterpräsentation: A new transgenic mouse model for sQTS without structural heart diseases. **Jänsch M**, Trum M, Williams T, Lubomirov LT, Schmitt J, Schuh K, Qadri F, Maier LS, Bader M, Ritter O

Zusammenfassung

In den letzten Jahren wurde in genomweiten Assoziationsstudien ein Zusammenhang zwischen Genpolymorphismen des Stickstoffmonoxid-Synthase-1 (NOS1) Adapterproteins (NOS1AP) und Variationen der Dauer des QT-Intervalls im EKG nachgewiesen. Krankheiten mit QT-Intervall Variationen, wie zum Beispiel das *long* QT Syndrom (LQTS), können ursächlich für einen plötzlichen Herztod sein. Das LQTS zeichnet sich durch eine verlängerte kardiale Repolarisation und eine daraus resultierende verlängerte Dauer des QT-Intervalls aus und bezeichnet neben der katecholaminergen polymorphen ventrikulären Tachykardie und dem Brugada Syndrom eine vererbbare Ionenkanalerkrankung. In Deutschland versterben jährlich etwa 65 000 Menschen am plötzlichen Herztod. Das sind ca. 20 % aller an Herzkreislauferkrankungen versterben Patienten (Martens et al., 2014). Eine Reduktion dieser hohen Sterblichkeitsrate ist weltweit Gegenstand der Grundlagenforschung.

Neben Mutationen in den kardialen Ionenkanälen selbst, kann auch die posttranslationale Modifikation dieser Ionenkanäle eine Rolle bei der Entstehung von Rhythmusstörungen spielen. Die S-Nitrosylierung bezeichnet eine posttranslationale Modifikation, bei der die Thiolgruppe von Cystein mittels Stickstoffmonoxid (NO) zu einem S-Nitrosothiol oxidiert wird. Das Enzym NOS1 katalysiert die Oxidation von L-Arginin zu L-Citrullin, wobei NO als ein ubiquitärer Botenstoff entsteht, der unter anderem auch bei der Regulation des Blutdrucks, Immunantwort und der neuronalen Kommunikation eine wichtige Rolle spielt. Die Co-Lokalisation von NOS1 zu den avisierten Targets ist abhängig von speziellen Adapterproteinen. Aufgrund der hochreaktiven Eigenschaften von NO, scheint speziell diese subzelluläre Lokalisation von NOS1 entscheidend für die NO-vermittelten Signalwege zu sein.

Erste Studien zur physiologischen Bedeutung von Nos1ap im Herzen wurden an Herzmuskelzellen von Meerschweinchen und HEK293 Zellen *in vitro* durchgeführt. Mit diesen Modellen konnte Nos1ap in Zellkultur über Proteinexpressionsanalysen im Herzen nachgewiesen werden. Nos1ap bindet über eine PDZ-Bindedomäne die Nos1 und wir vermuten, dass in dieser Kombination eine Co-Lokalisation zum L-Typ Calciumkanal (LTCC) stattfindet, verbunden mit einer Modulation der kardialen Elektrophysiologie.

In Vorarbeiten wurde bereits gezeigt, dass einer der oben erwähnten Genpolymorphismen (rs16847548), welcher in der Promoter-Region von NOS1AP lokalisierte ist, die Transkriptionsrate herabsetzt. In diesem Projekt wurde ein transgenes Mausmodell mit einer

induzierbaren und Herz-spezifischen Überexpression von Nos1ap erstellt und umfangreich charakterisiert.

Wir konnten die Bindung von Nos1ap an den LTCC und Nos1 bestätigen, diese Annäherung scheint die S-Nitrosylierung des Kanals zu begünstigen. Der LTCC ist die Hauptdeterminante für die Depolarisation des kardialen Aktionspotentials während der Plateau Phase 2 und beeinflusst so das QT-Intervall. Eine Immunpräzipitation mit den weiteren Calciumtransportern SERCA2a und PMCA4b konnte nicht nachgewiesen werden.

EKG-Messungen zeigten bei Mäusen mit verstärkter kardialer Nos1ap Expression ein verkürztes QT-Intervall (20 ± 1.9 vs. 28 ± 4.6 ms, $n = 6$, $p < 0.05$), außerdem neigten diese Tiere zu spontan auftretenden ventrikulären Tachykardien bis hin zum Kammerflimmern. In Langzeitexperimenten führte die induzierte Transgen-Überexpression zu einer gesteigerten Sterblichkeit von 40 % nach 100 Tagen. Mittels elektrophysiologischer Patch-Clamp-Messungen konnte eine verkürzte Dauer des Aktionspotentials nach 90 % der Repolarisation (APD_{90}) in isolierten Kardiomyozyten von induzierten Tieren festgestellt werden. Die Tiere mit kardialer Überexpression von Nos1ap zeigten keine strukturellen Herzveränderungen oder veränderten NT-proBNP Level, als Surrogat Parameter für Herzinsuffizienz. Letztendlich führte die kardiale Überexpression von Nos1ap zu einem *short* QT Syndrom mit letalen Tendenzen, ohne vorherige strukturelle phänotypische Auffälligkeiten in den Mäusen.

Zusammen mit Studien zur verringerten Promotoraktivität durch den SNP rs16847548 bestätigen die genannten Ergebnisse den Einfluss von NOS1AP auf die Elektrophysiologie des Herzens. Damit kann NOS1AP durch Modulation eines Ionenkanals als ein interessanter Wirkstoff-Angriffspunkt für die Behandlung von Herzrhythmusstörungen gesehen werden.

Summary

The QT interval duration is a defined part in the electrocardiogram (ECG), more specific the corrected QT interval (QTc) means correction by heart rate and reflects the ventricular repolarization. It may predispose individuals to ventricular tachycardia or sudden cardiac death (SCD) if prolonged, shortened or otherwise unregularly. Genome-wide association studies have linked genetic variations (single-nucleotide polymorphisms, SNPs) in the neuronal nitric oxide synthase 1 (NOS1) adaptor protein (NOS1AP) to variations in QTc and SCD.

NOS1 catalyzes the oxidation of L-arginine to L-citrulline and during that reaction nitric oxide (NO) emerges. NO acts as one of the most important ubiquitous signaling molecules for example in synaptic signaling, due to activation of guanylyl cyclase or by posttranslational modification of proteins (S-nitrosylation). We hypothesize that NOS1AP targets NOS1 to the L-type calcium channel (LTCC) leading to an inhibition of the channel via S-nitrosylation and thus affecting cardiac electrophysiology.

Transgenic FVB.N-Tg(TRE-Nos1ap)^{Jos} mice were mated with a second transgenic FVB.Cg-Tg(Myh6-tTA)6Smbf/J strain (The Jackson Laboratory) to generate double transgenic Nos1ap^{+}/αMHC-tTA^{+} mice with conditional overexpression of Nos1ap in cardiomyocytes (*Tet-off* expression system). Preliminary studies have examined the functional effect of the human SNP rs16847548 (T/C) located in the NOS1AP promoter region, which has been associated with QT interval prolongation. The SNP was found to decrease the transcriptional activity of NOS1AP *in vitro* and therefore, potentially, leading to a decrease of NOS1AP expression.

We investigated Nos1ap protein expression and localization using immunoblotting and immunocytochemistry in Nos1ap^{+}/αMHC-tTA^{+} mice. We confirmed the interaction of Nos1ap with Nos1 and LTCC and found no interaction with SERCA2a or PMCA4b. Electrocardiography in Nos1ap overexpressing Nos1ap^{+}/αMHC-tTA^{+} mice showed ventricular tachycardia and a significant decrease in QT interval duration (20 ± 1.9 vs. 28 ± 4.6 ms, n = 6, $p < 0.05$). Heart rates in NOS1AP overexpressing mice were similar to non-induced animals. Survival was significantly reduced (only 60 % after 12 weeks vs. 100 % in non-induced mice). No structural cardiac defects or changes in NT-proBNP levels, as indicator for heart failure (HF), were observed. Whole-cell patch-clamp measurements in isolated adult ventricular myocytes were performed and demonstrated shortening of the action potential duration at 90 % of repolarization (APD_{90}) in induced transgenic Nos1ap overexpressing mice compared to control littermates.

Finally, myocardial overexpression of Nos1ap leads to a short QT syndrome with increased susceptibility to ventricular arrhythmias and cardiac death. Together with reduced NOS1AP promoter activity of the human SNP rs16847548 obtained in preliminary studies, the results provide an explanation for the frequently published prolongation of the QTc interval. In summary, not only mutations in genes for ion channels but also genetic alterations in in genes coding for ion channel modulators such as NOS1AP, have an impact on QTc interval duration and arrhythmias.

1. Introduction

1.1. Regulation of EC Coupling for stable Heart Rate and a healthy Cardiovascular System

Excitation-contraction (EC) coupling in the heart is commonly seem as transformation of an electrical stimulus into a mechanical force – more specifically as transformation of action potentials (APs) into cardiac muscle contraction. The AP reaches the T-tubules in the sarcolemma of cardiomyocytes followed by extracellular calcium entry into the cells through voltage-gated L-type calcium channels (LTCCs). Likewise, that activates the ryanodine receptors (RyR) to release a much higher amount of calcium from the sarcoplasmic reticulum (SR) into the cytosol. That circle is called calcium-induced calcium release (Fabiato & Fabiato, 1979). The magnitude and rate of calcium release und uptake is crucial for intensity and frequency of cardiac contraction (Shiels & Galli, 2014).

The intracellular free calcium binds to the target protein troponin C and activates a signal cascade leading to conformational changes of troponin I and subsequently to activation of muscle contraction due to sliding of actin against myosin. Actin and myosin belong to the sarcomeric structure, which is the smallest part of the myofilaments. Actin and myosin are arranged in parallel, resulting in the characteristic striated form of the sarcomere (Li & Hwang, 2015). For cardiac contraction myosin heads move in presence of adenosine triphosphate (ATP) along actin filaments leading to cell shortening. That process is called cross-bridge cycling (A. M. Gordon et al., 2000).

On the other hand, the reuptake of cytosolic calcium for periodic relaxation followed by cross-bridge cycling is also important. The SR calcium ATPase (SERCA) transports calcium back to the SR. The release and reuptake of calcium in the SR calcium store is the main mechanism for a rapid change of intracellular calcium. The sodium/calcium exchanger (NCX) carrying 3 sodium ions into and 1 calcium ion out of the cell down an electrochemical gradient across the sarcolemma is less important for intracellular calcium homeostasis.

There are many other regulatory mechanisms for calcium handling in cardiomyocytes. For example, the two main modulators protein kinase A (PKA) and Calcium/calmodulin-dependent kinase II (CaMKII) enhance calcium influx via phosphorylation of LTCC, RyR and phospholamban (PLN, inhibitor of SERCA). CaMKII is a target for calcium and additionally influences specific transcription factors indirectly, resulting in repression of LTCC protein expression and moreover

upregulates NCX by different transcriptional regulation mechanisms (Dewenter et al., 2017). Accordingly, not only channel protein activation/inhibition via regulatory proteins and cellular organization but also expression levels of channel proteins are crucial for calcium cycling.

Dysregulation of calcium transients and signaling has immense consequences and is crucial in cardiac dysfunction. Lou et al. (2012) pointed out that enhanced CaMKII activity was correlated with impaired ejection fraction and a decreased amplitude of calcium transients in human failing heart. CaMKII also seems to be responsible for hyperphosphorylation of the RyR, leading to a higher SR calcium leak (Guo et al., 2006), despite other studies claiming the opposite (Yang et al., 2007).

1.2. Myocardial Electrophysiology

Cardiac electrical activation is initiated at the sinus node and conducted (top to bottom) to the atrioventricular node, bundle of His, right and left bundle branches and to the Purkinje fibers in the ventricles. The electrical cycle can be recorded in the electrocardiogram (ECG) representing different steps in form of different waves and segments transferred from a vector function of a defined heart axis. A typical sinus rhythm in the ECG includes the characteristic waves associated to defined phases (systole, diastole) of the heart cycle as shown in Figure 1. The P-wave is equivalent to the excitation of the atria, the QRS complex represents the ventricular depolarization and the T-wave indicates ventricular relaxation (Lewalter & Lüderitz, 2010).

Figure 1

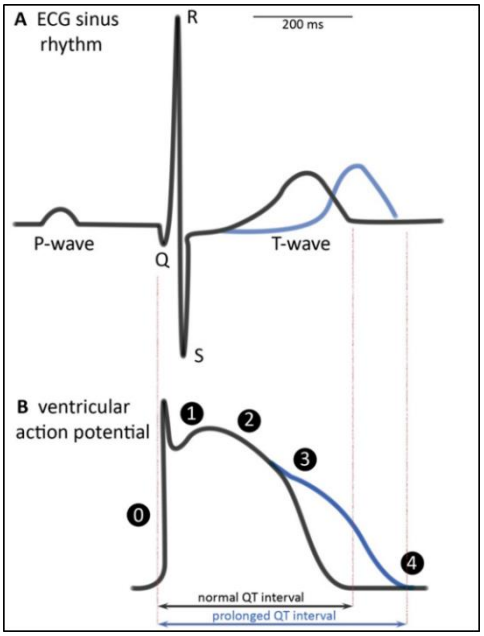

Legend to Figure 1. Drawing according to Grilo et al. (2010) of ECG sinus rhythm with typical PQRST waves and segments (A) and ventricular action potential with phase 0 to 4 (B). Blue colored lines represent pathological QT interval prolongation. Find further explanations in the text

Cardiomyocytes are electrically connected to each other via gap junction channels (connexins) and in general an AP activates as mentioned before (chapter 1.1) voltage-gated LTCCs for EC coupling and induces depolarization of the membrane by activation of different ion channels. In a physiological state electrical propagation is forwarded from cell to cell by connexins and is responsible for a periodic systole (contraction) and diastole (relaxation) heart cycle leading to constant pulsatile blood flow through the cardiovascular system.

Membrane depolarization in ventricular myocytes (Figure 1B, phase 0) starts with activation of the fast sodium inward current I_{Na} followed by fast repolarization (phase 1) due to I_{Na} inactivation and transient outward potassium (K) currents I_{to}. In phase 2 as a result of slow calcium inward currents $I_{Ca\text{-}L}$ the action potential forms a plateau until in phase 3 $I_{Ca\text{-}L}$ is terminated and the outward K currents I_{Kr} (r = rapid) and I_{Ks} (s = slow) further repolarize the membrane up to the additional I_{K1} activation and return to the resting membrane potential (phase 4) until a new AP reaches the cell (Lewalter & Lüderitz, 2010). Dysregulation of ion currents can lead to pathological QT interval prolongation (Figure 1) or other cardiac arrhythmias (Grilo et al., 2010).

1.2.1. Function and Regulation of the Open Probability of the L-Type Calcium Channel

As LTCCs are important for our investigations concerning the neuronal nitric oxide synthase 1 adaptor protein (NOS1AP) a short structural and functional overview is given.

LTCCs in cardiac myocytes influence on the one hand membrane repolarization by inward calcium currents $I_{Ca\text{-}L}$ during phase 2 of the AP in ventricular myocytes and that mechanism influences on the other hand the EC coupling as mentioned before in chapter 1.1.

LTCCs belong to the high-voltage-activated channels (HVA). Another common name is dihydropyridine receptor (DHPR) because of its sensitivity for dihydropyridine. It composes of the proteins named α_1 subunit, β subunit and the $\alpha_2\delta$ subunit (Hofmann et al., 1999).

The α_1 subunit is known to be most important for compound sensitivity (like calcium channel blockers) as well for voltage activation and selective directing of ions. The α_1 subunit contains four homologous transmembrane domains with hydrophilic N- and C-termini. The pore forming unit is located between the fifth and sixth transmembrane segment (S5 and S6) of each domain. The L-type class is divided in four subtypes ($Ca_V1.1$ – 1.4) depending on different genes coding

for the α_1 subunit. In the heart the α_1C subunit ($Ca_V1.2$) encoded by the *CACNA1C* gene is the most common isoform (Hofmann et al., 1999).

Beside the above-mentioned compound sensitivity there are different mechanisms for increasing or reducing the open probability of $Ca_V1.2$. Phosphorylation increases channel gating. The other subunits affect the velocity of channel activation for instance and even calcium regulates $Ca_V1.2$ in a negative feedback mechanism to prevent intracellular calcium overload (Hofmann et al., 1999).

Association studies found that genetic variations in the *CACNA1C* gene correlate with psychiatric disorders. The $Ca_V1.2$ isoform is also expressed in brain, here mainly in neurons of the hippocampus, cerebral cortex and cerebellum, indicating importance in neuronal signal conduction processes (Berger & Bartsch, 2014). Several rodent models with inducible or region specific knockouts of *Cacna1c* resulted in psychiatric phenotypes (Moon et al., 2018).

Tamara Hermosilla and her team found an angiotensin II dependent ~60 % reduction of $Ca_V1.2$ currents ($I_{Ca\text{-}L}$) and calcium flux in rat cardiomyocytes. They precisely describe the influence of β-arrestin$_1$ as it enhances internalization (equivalent with inactivation) of the channel. Therefore $Ca_V1.2$ currents are involved in angiotensin II driven cardiac remodeling (Hermosilla et al., 2017). Cardiomyocytes generate a cellular response by cardiac diseases and Pang et al. found in gene expression analysis a down-regulation of two isoforms of $Ca_V1.2$ by congestive heart failure (HF) diseases (Pang et al., 2003). These results indicate once more the relevance of alternative transcription rates of $Ca_V1.2$ caused by alterations in heart function due to a increased workload. Tester and Ackerman pointed out that mutations in the channel itself were considered to increase activity with higher calcium influx and higher membrane depolarization during the plateau phase 2 of the AP and subsequently AP prolongation as a consequence (Tester & Ackerman, 2014).

Beside the known major genes for LQTS, mutations in the gene *CACNA1C* were identified more frequently using next generation sequencing. Accordingly, *CACNA1C* now belongs to one of ~10 minor LQTS-susceptibility genes of the LQTS (Ohno et al., 2020).

1.3. Variation in the QTc Interval, Genetic Background and Acquired reasons

QT interval variations are caused by cardiac electrical disorders with prolongation or shortening of the QT interval on the ECG without structural heart diseases. In human species the QT interval differs in relation to heart rate (RR) and consequently usually the corrected QT (QTc)

interval is given after normalization with specific correction formulae (e.g. Bazett). Roussel and co-authors pointed out that there is no need for a QT interval correction in mice, as they found only weak relationship between RR and QT intervals (Roussel et al., 2016). QTc interval variations enhance the risk to suffer from ventricular tachycardia or fibrillation and sudden cardiac death (Bezzina et al., 2015). Notably *long* QT syndromes (LQTS) are clinical more relevant than *short* QT syndromes (SQTS). The LQTS can occur in inherited or acquired forms and females were more affected to suffer from cardiac events as a consequence of QTc interval prolongation (Zareba et al., 1995). Until now, mutations in up to 20 different genes are known to cause LQTS. The major three genes affected are *KCNQ1, KCNH2, SCN5A* and cover 75 % of genetic positive screenings in patients. The major LQTS genes (*KCNQ1, KCNH2, SCN5A*) are coding for potassium or sodium channel α subunits. Genes that are less frequently responsible for LQTS code for other ion channel subunits (e.g. potassium channel beta subunit or sodium channel beta 4 subunit) or other proteins with indirect impact on myocardial electrophysiology (e.g. calmodulin). Unfortunately 20 % of patients with pathologic QTc interval prolongation show no genetic variation in all of the ~20 LQTS-susceptibility genes suggesting an impact of other intra- or intercellular signaling mechanism (Tester & Ackerman, 2014).

From a clinical point of view LQTS often occurs in patients with an acquired prolongation of the QT interval as a consequence of negative drug side effects (Kang et al., 2001; Suessbrich et al., 1997). In the past, drugs that were tested in time- and money-consuming clinical trials had to be withdrawn from the market due to QTc prolonging side effects (Strobach et al., 2021). Frequently these drugs interfere with the potassium channel of the outward K currents I_{Kr} coded by *KCNH2*. Another naming of that channel is “human ether à-gogo related gene 1” (*hERG1*) related to the homolog gene found earlier in *Drosophila melanogaster*. As a consequence during drug development all compounds must pass preclinical hERG studies, before moving to phase I of clinical trials (Schwartz & Woosley, 2016; Grilo et al., 2010). Additionally, major efforts in research are put into the development of new assays for hERG1 interaction studies (Priest et al., 2008; Tang et al., 2001).

SQTS is much less studied and a rare familial disorder, nevertheless it is highly lethal. Only few pathogenic mutations were found in *KCNJ2, KCNQ1* and *CACNA1C* genes to explain this disease, characterized by accelerated repolarization, in most cases due to gain-of-function of hERG1 channels. Nevertheless, genetic screening has yielded much lower results compared to

screening for LQTS. Currently ICD implantation is the only therapy to protect individuals with pathologic SQTS from life-threatening events (Mazzanti et al., 2014).

1.4. Nitric Oxide Synthase Enzymes and NO Signaling in Heart

Ferid Murad and his group first described the function of nitric oxide (NO) in 1977, as a small, short-living radical gas, which easily diffuses across membranes. He demonstrated a NO induced activation of guanylate cyclase. That provided a basis for several further studies on additional NO dependent signaling mechanisms (Arnold et al., 1977). Later he was assigned the Nobel Prize for his research concerning that small molecule and until now we find many review articles (Bryan et al., 2009; Stamler et al., 1997) describing the influence of NO on physiological processes. A brief overview of the mentioned literature is given in the next section.

NO is produced by nitric oxide synthase (NOS) enzymes due to oxidation of L-arginine to L-citrulline in combination with the five co-factors calcium-calmodulin, heme, FAD, FMN and tetrahydrobiopterin. Another physiological NO donor is organic nitrite or nitrate used as NO storage form in tissues and blood. Three isoforms (NOS1, NOS2, NOS3) of the enzyme exists (Bryan et al., 2009) and NOS1 (alias for neuronal NOS) is considered to influence heart function due to cardioprotective effects and inhibition of cardiac contraction (Burkard et al., 2007; Burkard et al., 2010). Among others NO affects cardiac electrophysiology and finally EC coupling by nitrosylation of cardiac ion channels (Gonzalez et al., 2009). NOS1 and NOS3 are constitutive, cytosolic, calcium dependent and both were extensively studied in the neuronal and cardiovascular system. The NOS2 isoform is inducible, also cytosolic but calcium independent. NOS2 is activated by cytokines to modulate pro-inflammatory responses or in tumor necrosis factors. NOS2 activity is a biomarker for inflammation in tissues (Bryan et al., 2009).

Relaxation of smooth muscle cells and the related reduction of blood pressure is a well-known consequence of NO enrichment following increased NOS3 activity. Due to neuronal release of acetylcholine a second messenger system in the vascular endothelium is activated leading to activation of NOS3. Followed by diffusion of the produced soluble NO to the smooth muscle cells and induction of guanylate cyclase, vasorelaxation due to activation of protein kinase G (PKG) is mediated.

NO also inhibits platelet aggregation and thrombus formation. Activation of NOS3 in endothelial cells or of another platelet-specific NOS isoform (Muruganandam & Mutus, 1994) leads to NO production and a guanylate cyclase dependent increase of cGMP. The cGMP

activates PKG and cGMP-inhibited cAMP phosphodiesterase leading to platelet aggregation and adhesion decrease (Alonso & Radomski, 2003).

NO can also act guanylate cyclase independent by post translational modification of cysteine residues and conversion of thiol groups into S-nitrosothiols affecting protein function and signaling processes. Zou et al. found inhibitory effects due to enhanced S-nitrosylation of N-type calcium channels. Electrophysiological recordings were conducted using the NO donor S-nitroso-N-acetyl-DL-penicillamine (SNAP). To exclude other side effects of SNAP the same measurements were conducted with methanethiosulfonate ethylammonium (MTSEA) which modifies thiol groups to prevent conversion to S-nitrosothiols. MTSEA completely inhibits the effect of SNAP on the channel and confirms hereby the postulated mechanism of S-nitrosylation (Zhou et al., 2015). Gonzalez et al. pointed out that dysregulation of syntrophin was associated with LQT3, by enhancing the interaction of NOS1 with the sodium channel coded by *SCN5A* and promoting nitrosylation of the channel. In that case the nitrosylation led to enhancement of late sodium currents and prolongation of the QT interval (Gonzalez et al., 2009). Another NOS1 interacting protein called NOS1AP was identified in numerous studies (Crotti et al., 2009; Kolder et al., 2015; Sugiyama et al., 2016; Tomas et al., 2010; Zang et al., 2019; Zhang et al., 2017) to influence QTc interval duration. In cell culture experiments Chang et al. found that NOS1AP interact with NOS1 and LTCC. Overexpression of NOS1AP led to inhibition of the calcium channel possibly due to enhanced S-nitrosylation as NOS1AP translocates NOS1 to LTCC. They found shortening of APD_{90} as inhibition of LTCC led to a faster repolarization in phase 2 of the AP in cardiomyocytes (Chang et al., 2008). Other investigations concerning Nos1ap demonstrated a co-localization of Nos1ap with Nos1 after myocardial infarction (MI). Here, in cardiomyocytes of wildtype mice isolated post-MI, Nos1ap together with Nos1 translocated to the plasma membrane to protect cells from toxic intracellular calcium levels due to S-nitrosylation of LTCC. In contrast, in post-MI Nos1 knockout mice there was no migration of Nos1ap. It appears that the transport of NOS to subcellular destinations is important for the effect of NO signaling and the amount of S-nitrosylation of target proteins (Beigi et al., 2009). In that context it is interesting that exclusively the isoform NOS1 contains a PDZ binding domain similar to NOS1AP. Obviously, the PDZ domain determines the subcellular targeting of the adjacent proteins. Noteworthy, Treuer and Gonzalez assessed the relevance of Nos1ap using RNA silencing (siRNA) technology in neonatal rat cardiomyocytes. They found interactions of Nos1ap with LTCC and other ion channels regulating the AP duration. Silencing

Nos1ap reduced calcium transient amplitude and S-nitrosylation of the cells. They concluded that NOS1AP has an impact on cardiac arrhythmias as is was up-regulated in mice with dystrophic cardiomyopathy (Treuer & Gonzalez, 2014).

Cardio protective effects are a result of the ability of NO to modulate the redox state. NOS is relevant to keep the normal nitroso-redox balance, which means the balance between reactive oxygen species (ROS) and NO. Oxidative stress can influence cardiac health in a negative manner. Recent data revealed a connection between the antioxidant effect of exercise and Nos1 in mouse hearts. Nos1 knockout mice revealed much higher ROS levels and a contractile dysfunction compared to wildtype mice with intact Nos1 activity after exercise. They also tested transgenic mice with a heart-specific Nos1 overexpression and found a decrease of ROS levels, enhanced contraction in myocytes and furthermore enhanced heart function *in vivo* after treadmill training (Roof et al., 2015). Burkard et al. demonstrated the same myocardial protection after ischemia/reperfusion injury and also decreased ROS levels in another Nos1 overexpressing mouse model (Burkard et al., 2007). Furthermore, they found a decrease in myocardial contractility und a decline in the calcium transient amplitudes due to inhibition of LTCC (Burkard et al., 2010).

1.5. Preliminary Data and Aim of this Project

Contemporary studies have identified genetic variants (single nucleotide polymorphism, SNP) in the *nitric oxide synthase 1 (NOS1) adaptor protein (NOS1AP*) gene leading to variations in QTc interval duration (Aarnoudse et al., 2007; Kolder et al., 2015; Zhang et al., 2017).

The aim of this project was to determine the impact of Nos1ap and regulatory mechanisms concerning QT variation in the whole organism by using a conditional Nos1ap overexpression mouse model.

In earlier studies of our group a similar transgenic mouse model with inducible overexpression of Nos1 was established and characterized with focus on myocardial contractility. Beside reduced contractility and ejection fraction, a Nos1 dependent decrease of L-type calcium channel current ($I_{Ca\text{-}L}$) density in Nos1 overexpressing animals was found (Burkard et al., 2007; Burkard et al., 2010).

Figure 2A depicts the possible NOS1-NOS1AP-LTCC interaction (Beigi et al., 2009; Treuer & Gonzalez, 2014). We here followed the hypothesis (supported by earlier results) that Nos1ap is crucial to cause co-localization of Nos1 and LTCC and consequently a lower proximity to the

LTCC, yielding in inhibition of the channel activity with a subsequent influence on cardiac electrophysiology.

Chang and his group demonstrated the function of Nos1ap as it up-regulates the Nos1-NO signaling cascade with impact on $I_{Ca\text{-}L}$ in isolated cardiomyocytes *in vitro*, but they were lacking the proof-of-principle in a whole organism system (Chang et al., 2008). Another group around Treuer and Gonzalez investigated the effect of Nos1ap silencing in neonatal cardiomyocytes leading to lower degree of S-nitrosylation in cells and changed calcium transients. They found an up-regulation in mice with cardiac arrhythmias as well (Treuer & Gonzalez, 2014).

For a better understanding of Nos1ap dependent signaling and interaction in a complete physiological system in comparison to the mentioned data from cell culture, in previous experiments founder mice with a pTRE-6HN-Nos1ap plasmid genetic background were generated. These mice are characterized by an inducible heart-specific overexpression of Nos1ap using a *Tet-Off* system. The functionality of the *Tet-Off* system was proven with a HEK293 *Tet-Off* Advanced Cell Line (Clontech) and by transfection with the pTRE-6HN-Nos1ap vector construct. Cancelling the doxycycline substitution from culture media upregulated Nos1ap expression, what has been demonstrated in western blots. The sperms of the obtained transgenic mice were cryopreserved for the subsequent revitalization within the context of this PhD thesis.

First results using the generated Nos1ap overexpression mouse model could confirm a cardiac co-localization of Nos1ap, Nos1 or LTCC respectively (Figure 2B) and resulted in higher interaction of Nos1ap with Nos1/LTCC due to overexpression of Nos1ap in transgenic mice compared to controls.

Figure 2

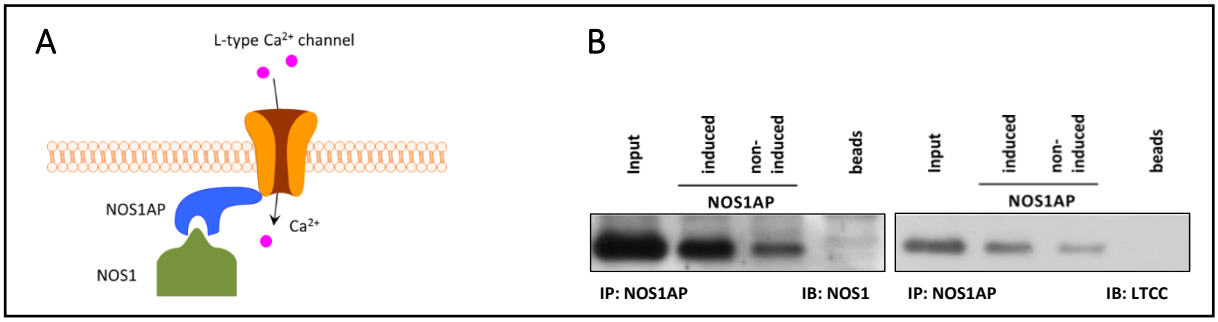

Legend to Figure 2. Simplified schematic drawing of the NOS1-NOS1AP-LTCC interaction (A) and co-localization studies of Nos1ap and Nos1 or LTCC in both, induced Nos1ap overexpressing and non-induced mice. Nos1ap overexpression resulted in a higher co-reactivity compared to non-induced littermates (B)

The QT interval in the ECG describes the time between the beginning of the QRS complex and the end of the T-wave and reflects ventricular de- and repolarization. It may predispose individuals to ventricular tachycardia and sudden cardiac death (SCD) if prolonged, shortened or otherwise unregularly. QTc interval prolongation is caused by inherited or acquired reasons (Amin et al., 2010).

Since genome-wide association studies recently linked genetic variations in NOS1AP to QTc variations in otherwise healthy individuals, in addition investigations concerning the functional effect of the human SNP rs16847548 (T/C) which is located within the NOS1AP promoter region were conducted in preparation of this project. Gene expression was analyzed in neonatal rat cardiomyocytes by a luciferase reporter assay with a pGL3-Promoter vector (Promega) containing the ~4kb human NOS1AP element with the SNP rs16847548 upstream of the luciferase gene. As control the wildtype NOS1AP element was utilized. Luciferase activity was measured with a luminometer and results showed this SNP significantly impairs promoter activity resulting in less transcriptional activity *in vitro* (Figure 3).

Figure 3

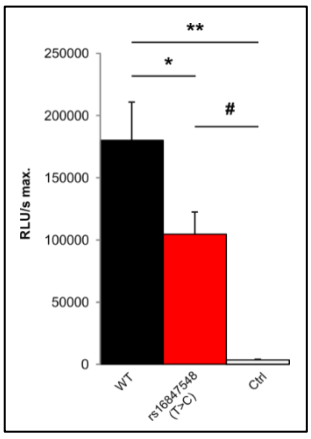

Legend to Figure 3. Luciferase assay. The mutated promoter, carrying the minor allele of SNP rs16847548 (T/C) leading to decreased NOS1AP promoter activity in a viral NOS1AP luciferase assay, suggesting that this SNP suppresses NOS1AP expression in humans

One previous study was published concerning the function of NOS1AP in whole organism, but in contrast to this work the focus was here on oxidative stress in Nos1ap deleted mice. They found no electrocardiographic changes in mice with deletion of Nos1ap under baseline conditions, but after exposure to oxidative stress with doxorubicin injection longer QT intervals and higher mortality compared to wildtype mice were seen (Sugiyama et al., 2016). Another recent study hypothesized that NOS1AP SNPs causes NOS1 dysfunction correlated to QT prolongation. The authors found an independent QT interval prolonging mechanism due to inhibition of Nos1 or I_{Ks} (*KCNQ1*, LQT1) respective and furthermore enhanced calcium inward

currents $I_{Ca\text{-}L}$ due to Nos1 inhibition in guinea pig cardiomyocytes. Besides, they showed in induced human pluripotent stem cell-derived cardiomyocytes (hiPSC-CMs) of LQT1 patients with major and minor allele of NOS1AP that the minor allele of NOS1AP led to decrease of NOS1AP and NOS1 expression in symptomatic LQT1 patients resulting in a larger peak $Ca_V1.2$ density (Ronchi et al., 2021). That supports our idea of NOS1 dependant inhibition of LTCC ($Ca_V1.2$) and through the suggested impact of NOS1AP. We hypothesize that Nos1ap has a modulator function on the open probability of the LTCC. Further we suggest that variation in Nos1ap protein expression is of relevance for the QT interval duration.

2. Material and Methods

All chemicals used were purchased from the companies CARL ROTH, VWR Chemicals, SERVA, Merck Millipore or Sigma-Aldrich® unless otherwise marked. Statistical evaluation for significant differences between paired respective unpaired variables were calculated using t-test with the SPSS statistics (IBM) software. Values were given by means including standard deviation (± SD) and the Pearson correlation coefficient was applied.

2.1. *Tet-Off*-regulated Mouse Model

The working group of Professor Oliver Ritter established the transgenic mice model used for this research project. A pTRE-6xHN vector (Clontech Laboratories, Cat. No. 631009 vector information material, Figure 4A) was selected to use the tetracycline-regulated gene expression system named *Tet-off* (Gossen & Bujard, 1992). The cDNA sequence (1.509 kb) coding for the murine Nos1ap protein Isoform 1 (Organism: *Mus musculus*, see appendix A2 for full sequence) was inserted in the multiple cloning site (MCS) in-between the restriction sites *Hind* III and *Xba* I. Figure 4 shows structural information of the pTRE-6xHN vector without (A) and with (B) insert.

Figure 4

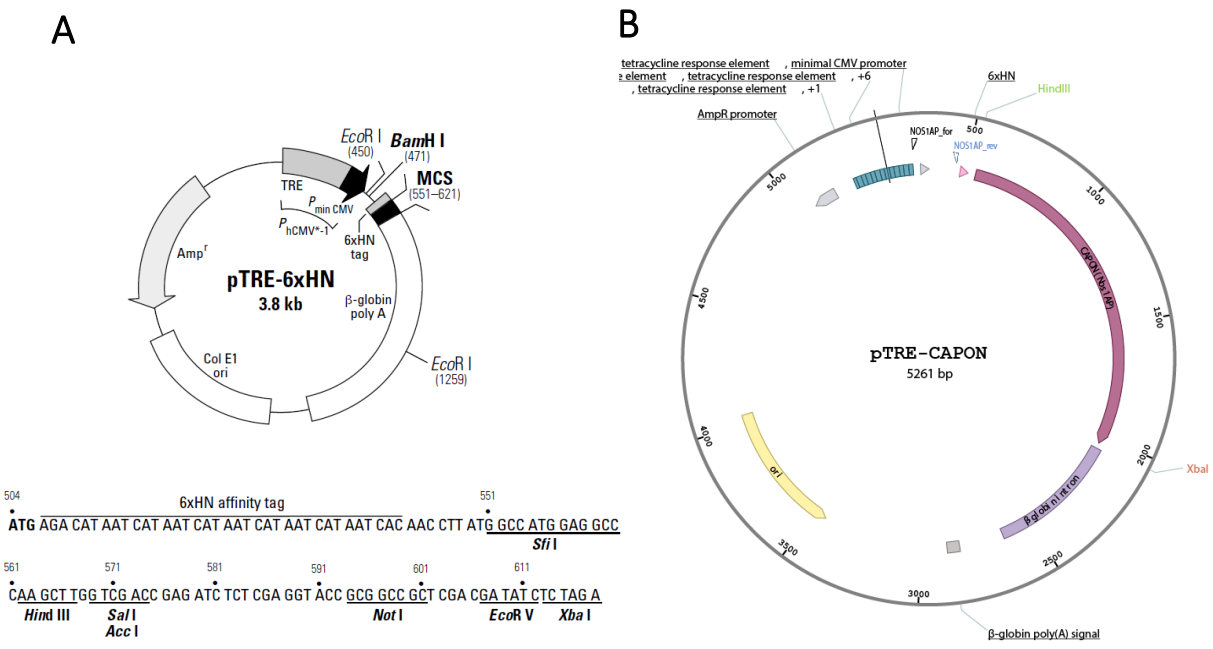

Legend to Figure 4. Map of used pTRE-6xHN vectors without (A) and with (B) insert. (A) pTRE-6xHN is a tetracycline response plasmid (Clontech Laboratories) that can be used to tag a gene of interest with a 6xHN affinity tag and to induce expression of the insert depending on activation of the tet-responsive element (TRE). It also contains a multiple cloning site (MCS) downstream TRE and upstream the ß-globin poly A intron to allow splicing of the expressed insert, an origin of replication (ori) and an ampicillin resistance gene (*Ampr*). (B) Capon (Nos1ap) coding sequence is inserted to the MCS of pTRE-6xHN vector between *Hind III* and *Xba I*. Vector-specific primers for genotyping are included (see appendix A2 for full sequence)

The constructed *Tet-off* vector system was sequenced and tested in HEK 293 cells and verified with western blot analysis. To generate transgenic founders the pTRE-6HN-Nos1ap vector was microinjected to the pronuclei of fertilized FVB/N mouse oocytes (J. W. Gordon et al., 1980). To obtain mice with conditional overexpression of the target gene in ventricular cardiomyocytes (*Tet-off* system), mice were mated with a second transgenic FVB.Cg-Tg(Myh6-tTA)6Smbf/J strain (The Jackson Laboratory). That second strain expresses the tetracycline-controlled transactivator protein (tTA) under the regulatory control of the rat alpha myosin heavy chain promoter (description of JAX stock #003170) which is expressed predominantly in the human atria (Reiser et al., 2001) and in adult murine hearts (Ng et al., 1991). Individuals with genetic background of both strains are indicated as double transgenic (DT) Nos1ap^{+}/αMHC-tTA^{+} mice. In Figure 5A the breeding diagram of both heterozygous strains is depicted. Breeding results in a ratio of 75 (other) to 25 (DT mice). By application of a doxycycline diet, the doxycycline binds to tTA and that is why activation of the tet-responsive element (TRE) is prevented. Application of a standard diet leads to heart-specific overexpression of Nos1ap due to activation of TRE by binding of tTA (Figure 5B).

Figure 5

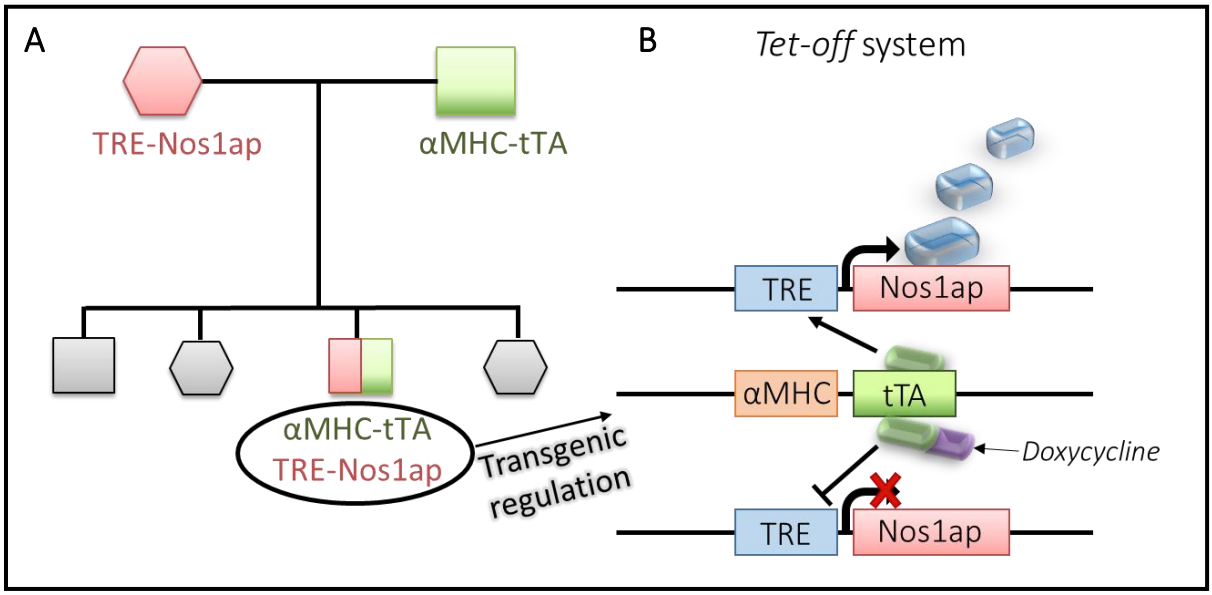

Legend to Figure 5. Breeding diagram of used heterozygous strains (A). TRE-Nos1ap: FVB.N-Tg(TRE-Nos1ap)^{Jos} strain, αMHC-tTA: FVB.Cg-Tg(Myh6-tTA)6Smbf/J strain. Transgenic regulation mechanism of the *Tet-off* system in double transgenic mice with/without doxycycline diet (B). TRE: tet-responsive promoter element, Nos1ap: neuronal nitric oxide synthase 1 adaptor protein, αMHC: alpha myosin heavy chain promoter, tTA: tetracycline-controlled transactivator protein

Sperms of the transgenic FVB.N-Tg(TRE-Nos1ap)^{Jos} founder mice (Nos1ap^{+}/αMHC-tTA^{-} mice) were cryopreserved for long term storage and revitalization.

The Institutional Animal Care and Use Committees at the Centre for Experimental Molecular Medicine Wuerzburg (ZEMM, AZ: 55.2-2531.01-53/11) and the Regional Office for Health and Social Affairs Berlin (LAGeSo, AZ: G 0105/18) approved the animal experiments for that project. Main experiments were conducted from August, 2018 for four years onwards with an extent of 236 mice at Max-Delbrück-Center for Molecular Medicine in the Helmholtz Association (MDC) in Berlin and at Brandenburg Medical School at the Biomedical Research Center Brandenburg (ZTM-BB) in Brandenburg/Havel (AZ: 2347-12a-2021). All experiments with mice were performed in accordance with the guidelines of German Animal Welfare Act for a good care and use of laboratory animals.

2.2. Animals and Housing Conditions

The used FVB/NJ Mice strain is suitable for genetic modification, because of the prominent pronuclei in its fertilized eggs and that is suitable for handling the pronuclear injection of plasmid DNA to generate the transgenic founders. The cryopreserved sperms of transgenic Nos1ap^{+}/αMHC-tTA^{-} founders were revitalized by *in vitro* fertilization by the transgenic core facility (TCF) and subsequent breeding was realized at the MDC in collaboration with Professor Michael Bader.

As mentioned before a *Tet-off* mouse model was used, hence the DT mice got a special doxycycline (100 mg/kg food) diet starting from birth. For inducing the overexpression of Nos1ap the feeding changed from doxycycline to a standard diet without doxycycline ten days before starting measurements. As a control non-induced DT and Nos1ap^{+}/αMHC-tTA^{-} mice were utilized.

All mice were bred and housed under specific pathogen free (SPF) conditions following the Federation of European Laboratory Animal Science Associations (FELASA) standards in individually ventilated cages (IVC). SPF is defined as an environment free of specific listed pathogens with sentinel controls by serological tests. SPF housing is recommended to obtain comparable results in the best possible way. Nevertheless, infections can occur despite the absence of clinical diseases, resulting in experiments negatively influenced by change of behaviour, reduced breeding efficiency or sample contamination. SPF housing saves animals as

lower sample numbers are needed and finally takes into account animal welfare (Kunstyr & Nicklas, 2000).

Experiments were started at the age of 10 to 16 weeks. Considering the poor yield of cross breeding of two heterozygous strains with a ratio of 75 (other) to 25 (DT mice) male and female subjects had to be used, regardless of the hormonal influence on cardiac electrophysiology.

To take into account the physical, physiologic and behavioral needs of the species *Mus musculus* the room temperatures was adjusted to 23°C with a 12/12 h circadian rhythm. The mice lived in small groups of 4 – 6 animals with nesting material, appropriate housing space and access to water/food *ad libitum*. Cages were changed frequently and a score sheet was used for routine monitoring of health.

2.3. Genotyping by Polymerase Chain Reaction (PCR)

In accordance with animal welfare ear biopsy was taken for labeling and simultaneously for the isolation of DNA for genotyping. Genotyping was kindly done at the MDC and checked after sacrificing the animals in own laboratory conditions.

For genotyping DNA was extracted with the genomic DNA isolation kits, XIT for mouse tail (G-Biosciences) according to manufacturer's instructions. DNA concentration and contamination was measured with NanoDrop One (Thermo Scientific). For PCR product amplification the *Taq* DNA Polymerase (Qiagen) was used by preparing the following reaction mix on ice: 2 µl 10x PCR Buffer, 0.4 µl 10 mM dNTP Mix (Thermo Scientific), 0.5 µl *Taq* DNA Polymerase, 0.8 µl 25 mM $MgCl_2$. For genotyping the Nos1ap transgen in mice 0.3 µl NOS1AP3 and 0.3 µl NOS1AP5 primer and for αMHC-tTA 0.4 µl oIMR8744, 0.4 µl oIMR8745, 0.3 µl oIMR8746 and 0.3 µl oIMR8747 were pipetted separately to the reaction mix (find oligonucleotide sequences of primers in Table 1). Finally, 100 ng template DNA and RNAse-free water was added to total reaction volume of 20 µl.

The PCR was performed with the thermocycler peqSTAR (Peqlab a VWR brand) following two different programs, depending on primer combinations (Table 2). For identification of $Nos1ap^+$/$\alpha MHC\text{-}tTA^+$ mice genotyping with same DNA was run twice; one with NOS1AP3/5 and one with Tg(tTA) primer combinations.

To analyze the PCR product an electrophoresis (100 V for 1 h) with a 2 % agarose gel (50 ml 1x TAE buffer, 1 g agarose) was performed. A 10x stock of TEA running buffer composed of 0.4 M Tris-acetate and 0.01 M EDTA solved in deionized water was used. The samples for

electrophoresis were mixed with 6x loading dye solution (Thermo Scientific) and 10x GelRed nucleic acid gel stain (Biotium). Afterwards they were loaded on the gel as well as a 50 bp peqGOLD ladder (VWR Chemicals).

Table 1. Oligonucleotide sequences of used primers for PCR genotyping

Primer	Sequence 5' → 3'	Primer type	Product size (bp)	Reference
oIMR8744	CAAATGTTGCTTGTCTGGTG	Internal positive control forward	200	Protocol Tg(tTA) Jackson Laboratory
oIMR8745	GTCAGTCGAGTGCACAGTTT	Internal positive control reverse	200	Protocol Tg(tTA) Jackson Laboratory
oIMR8746	CGCTGTGGGGCATTTTACTTTAG	Transgene tTA forward	450	Protocol Tg(tTA) Jackson Laboratory
oIMR8747	CATGTCCAGATCGAAATCGTC	Transgene tTA reverse	450	Protocol Tg(tTA) Jackson Laboratory
NOS1AP3	CGTCAGCTGACTAGAGGATC	pTRE-6xHN-Nos1ap_reverse	201	Michael Bader (see Figure 4)
NOS1AP5	TGAAAGTCGAGCTCGGTACC	pTRE-6xHN-Nos1ap_forward	201	Michael Bader (see Figure 4)

Table 2. Cycling conditions for the PCR genotyping

FVB.N-Tg(TRE-Nos1ap)^{Jos}			FVB.Cg-Tg(Myh6-tTA)6Smbf/J		
Step	Time	Temperature	Step	Time	Temperature
Initial denaturation	3 min	94°C	Initial denaturation	2 min	94°C
3-step cycling			**3-step cycling**		
Denaturation	30 sec	94°C	Denaturation	20 sec	94°C
Annealing	30 sec	60°C	Annealing	15 sec	65°C
Extension	40 sec	72°C	Extension	10 sec	68°C
Number of cycles	**40**		**Number of cycles**	**10**	
Final extension	5 min	72°C	Note	-0.5°C decrease per cycle	
	hold	*10°C*			
			3-step cycling		
			Denaturation	15 sec	94°C
			Annealing	15 sec	60°C
			Extension	10 sec	72°C
			Number of cycles	**28**	
			Final extension	5 min	72°C
				hold	*10°C*

2.4. Characterization of DT Mice compared to Control Littermates

For determination of the survival rate, mice of different groups (n = 20; induced DT and for controls non-induced DT and Nos1ap^{+}/αMHC-tTA^{-} mice) were monitored for 100 days and afterwards phenotyped by measuring the heart- and bodyweight and additionally the weight of brain, liver, spleen, kidney and lung. All organs were transferred in dry ice tempered 2-methylbutane followed by long-time storage at –80°C. In contrast to the other organs the tops of hearts were processed in another way for paraffin-embedding and structural analysis (see Section 2.4.4.). To confirm heart-specific overexpression of Nos1ap in DT mice compared to controls, heart tissue of mice with induction respective non-induction of overexpression ten days before sampling was stored at – 80°C for subsequent analysis.

2.4.1. Isolation of Ventricular Myocytes for Patch-Clamp and Protein Expression Analysis

The isolation was kindly done in collaboration with the University Hospital Regensburg. For isolation of adult cardiomyocytes mice were cervical dislocated by trained individuals. The heart was isolated immediately and transferred to cold (4 ± 1°C) tyrode solution (ingredients in Table 3) and the aorta was rapidly cannulated by fixing with surgical supramid suture material (Serag-Wiessner, SUPRAMID, size 5/0) using a stereo microscopes SZ61 (Olympus). The heart was retrogradely perfused with a tempering container and a heat exchanger (Gebr. Rettberg GmbH, Göttingen) according to Langendorff connected to a peristaltic pump (Rainin Dynamax, 4 ml/min) for constant temperature management (Figure 6).

Figure 6

Legend to Figure 6. Picture of the tempering container and heat exchanger (Gebr. Rettberg GmbH, Göttingen) according to Langendorff with cannulated heart for isolation of cardiomyocytes

Due to retrogradely perfusion the cold solution flows in opposition to normal physiologic direction in the aorta. Thus the aortic valve is closed and tyrode is flowing around the heart via the coronary vessels without filling the ventricle (Bell et al. 2011). For that the Langendorff apparatus was loaded with the cold (6.2 ± 0.2°C) tyrode solution (without bubbles) followed by the lyse solution (20 ml tyrode solution, 0.75 mg Liberase TM (Roche), 100 µl of 10x Trypsin (2.5 %, Gibco) and 25 µl of 10 mM $CaCl_2$). The cannulated heart was perfused for 2 min by tyrode solution followed by 6 min lyse solution. Atria were separated with a scissors. Thereafter mechanical cell digestion was prepared in a petri dish filled with stop solution (2.25 ml tyrode solution, 250 µl Bovine calf serum, 3.125 µl 10 mM $CaCl_2$). Isolated cardiomyoytes were filtered through a membrane (pore size 115 × 145 µm) to remove dead tissue material. For a stepwise (8 min/step) increase of calcium (0.1, 0.2, 0.4, 0.8 mM) a 100 mM $CaCl_2$ solution was diluted in the tyrode solution with addition of 5 % bovine calf serum. Final calcium concentration depends on used bath solution for whole-cell patch-clamp measurements (for this project it contains 1 mM $CaCl_2$). Find in Table 3 the used ingredients of tyrode solution for heart perfusion according to Langendorff.

Table 3. Ingredients of 1x tyrode solution and needed 50x BDM stock solution

Final concentration	Ingredients
113 mM	Sodium chloride NaCl (58.4 g/mol)
4.7 mM	Potassium chloride KCl (74.6 g/mol)
0.6 mM	Potassium dihydrogen phosphate KH_2PO_4 (136.1 g/mol)
0.6 mM	Sodium phosphate, dibasic heptahydrate Na_2HPO_4 x $2H_2O$ (177.99 g/mol)
1.2 mM	Magnesium sulfate heptahydrate $MgSO_4$ x $7H_2O$ (246.48 g/mol)
32 µM	Phenol red (354.376 g/mol)
12 mM	Sodium hydrogen carbonate $NaHCO_3$ (84.01g/mol)
10 mM	Potassium hydrogen carbonate $KHCO_3$ (100.12g/mol)
10 mM	2-[4-(2-hydroxyethyl)piperazin-1-yl]ethanesulfonic acid HEPES (238.31 g/mol)
30 mM	Taurine (125.1 g/mol)
1x	2,3-Butanedione monoxime BDM (use 50x BDM Stock Solution)
Ad deionized water and store at 4°C, for a plenty of experiments a 10 x stock is recommended	
50x BDM stock solution	
500 mM	2,3-Butanedione monoxime BDM (101 g/mol)
Ad deionized water, heat solution to prevent precipitation, store stock solution in aliquots at -20 °C	

2.4.2. Protein Expression and Co-Immunoprecipitation Analysis

Protein Extraction

Isolated ventricular cells or tissue (~10 mg) was homogenized for 15 min on ice by using a pellet micro pestle (Eppendorf). The homogenization took place in 600 µl lysis buffer containing 300 NaCl, 100 NaH2PO4 x H2O, 10 Na4P2O7, 1 MgCl2 x 6 H2O, 50 Na2HPO4 and 10 EDTA (mM, pH 7.4) plus freshly added 1 mM phenylmethylsulfonyl fluoride (PMSF, 100 mM stock solution in isopropanol), PhosSTOP phosphatase inhibitors (Roche) and cOmplete protease inhibitors (EDTA-free, Roche). To discard cell residues, samples were centrifuged at 21 000 x g for 5 min at 4°C and supernatant with proteins were transferred to a new reaction tube and immediately stored at – 80°C (long time) or -20°C (short time) to prevent protein degradation.

Protein Quantification

Total protein concentration was determined by using the Bradford (Bradford, 1976) colorimetric assay. The used dye reagent (Bio-Rad) includes Coomassie brilliant blue what interacts with proteins followed by absorbance shift in cause of ionic interactions. The amount auf proteins is proportional to alteration of red to blue color of the dye. Protein concentration were colorimetrically measured with a spectral photometer SmartSpec 3000 (Bio-Rad) at λ = 595 nm (A595).

The working solution (WS) of dye reagent (Bio-Rad) was diluted in a 1 to 5 ratio. Total volumes were calculated by mixing WS, distilled water (dH2O) and a 1 mg/ml stock solution of BSA in dH2O as shown in Figure 7. For interpretation a standard curve was created (Figure 7) with defined protein concentrations of bovine serum albumin (BSA). To determine the protein concentration 2 µl of protein sample were mixed with 18 µl dH2O and 980 µl WS and measured at A595. By using the obtained regression equation (y = 0,0586x + 0,052) the defined protein concentration was calculated. As we use 2 µl sample volume the correct protein concentration was obtained by halving the results.

Figure 7

BSA (mg/ml)	A595	Total volume
0	0	20 µl dH_2O + 980 µl WS
1	0,096	1 µl BSA stock + 19 µl dH_2O + 980 µl WS
2	0,179	2 µl BSA stock + 18 µl dH_2O + 980 µl WS
4	0,279	4 µl BSA stock + 16 µl dH_2O + 980 µl WS
6	0,425	6 µl BSA stock + 14 µl dH_2O + 980 µl WS
8	0,527	8 µl BSA stock + 12 µl dH_2O + 980 µl WS
10	0,623	10 µl BSA stock + 10 µl dH_2O + 980 µl WS

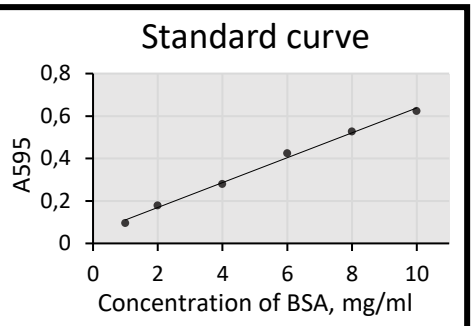

Legend to Figure 7. Values and chart for standard curve calculation for Bradford assay with linear regression curve and equation y = 0,0586x + 0,052. A595 denotes absorption at 595 nm wavelength

SDS-PAGE and Gel Staining

The Mini-PROTEAN Tetra electrophoresis system and Mini Trans-Blot Cell system (Bio-Rad) was used for separation of proteins by molecular masses (SDS-PAGE). Handcast polyacrylamide gels were prepared using the Invitrogen SureCast resolving and stacking buffer (Thermo Fisher Scientific). The solution of one resolving gel contains 2 ml SureCast resolving buffer, 2.67 ml ROTIPHORESE Gel 30 (2.7 % crosslinker concentration), 3.23 ml dH2O, 80 µl ammonium persulfate (APS, 10 %) and 8 µl tetramethylethylenediamine (TEMED). Polyacrylamide gels are characterized by polymerization of two monomers by adding APS for oxidization and TEMED for catalysis of polymerization. Pore size of the gel is negative proportional to the crosslinker concentration. The solution of one stacking gel contains 0.75 ml SureCast stacking buffer, 0.4 ml ROTIPHORESE Gel 30, 1.82 ml dH2O, 30 µl APS (10 %) and 3 µl TEMED. Handcast gel preparation was conducted in accordance with the Bio-Rad user manual using the casting stand assembly and 1.5 mm gel thickness. The resolving gel had to be coated with water and incubated for 1 h for complete polymerization before pouring the stacking gel. Finally, we obtain a 10 % resolving and 4 % stacking gel ready to use for SDS-PAGE.

The gels were loaded with a protein concentration of about 10 to 20 µg per lane. Previously each sample was diluted in Laemmli sample buffer (4x) containing 200 Tris PUFFERAN, 400 dithiothreitol (DTT), 8 % sodium dodecyl sulfate (SDS) pellets, 40 % glycerol and 0,04 % bromophenol blue (mM, pH 6.8). Then the samples were heated for 5 min at 95°C for denaturation before gel loading. 3 µl of prestained protein marker (10 – 245 kDa; Applichem Lifescience) were used for determination of protein size. By using the PowerPac HC Power Supply (Bio-Rad) the SDS-PAGE moved into a running buffer containing 25 mM Tris PUFFERAN, 190 glycine and 0.1 % SDS (mM, pH 8.3) for 2.5 h. The process began at 70 V for 10 min until

the samples reached the resolving gel. Afterwards, the SDS-PAGE moved at a constant voltage of 100 V from negative to positive pole, until the dye front entered the bottom of the gel.

SDS is an anionic detergent composed of hydrophobic and hydrophilic parts for integration to lipid bilayer structures, like biological membranes. In this manner membrane-bound proteins were solubilized. Due to interaction, it helps together with DTT (reduces disulfide crosslinks) to unfold proteins to its primary protein structure. Additionally, SDS masks by binding all charged groups of the proteins and transforms them to negative charge.

For visualization of sample quality, gels were stained for 1 h in Coomassie brilliant blue R250 solution containing 0.2 % blue, 40 % ethanol and 7.5 % acetic acid in water (reusable). To see protein bands afterwards the gel must be bleached overnight in a solution containing 20 % methanol and 7.5 % acetic acid in water (reusable).

Western Blot and Immunodetection

By using the Mini Trans-Blot Cell system (Bio-Rad) the proteins were transferred to a 0.45 µm PVDF (Amersham Hybon) membrane (constant 17 V, 14 h). The blotting buffer containing 25 boric acid and 2 EDTA (mM, pH 8.8) in water. Before blotting PVDF membrane was activated in methanol for 1 min. Protocol optimization was conducted for each antibody by correcting the incubation time and antibody concentration resulting in following protocol depicted in Table 4. PVDF membranes with bound proteins were washed for 10 min in TBST/BSA (Tris-Buffered Saline containing 0.15 M sodium chloride, 10 mM tris base and 0.1 % Tween 20 with 0.1 % BSA, pH 8) followed by 1 h blocking in 10 % powdered milk diluted in TBST at room temperature (RT).

Especially for proteins with a low amount in the total sample volume, another procedure was established and performed before staining with primary antibodies. In short; membrane washing for 10 min in TBST/BSA, followed by 5 min blocking in TBST with 1 % BSA and 1 % powdered milk, followed by another washing in TBST/BSA and immobilization for 15 min in 0.2 % glutaric dialdehyde, short washing in TBST/BSA and finally blocking in TBST with 1 % BSA and 1 % powdered milk for 1 h.

Primary antibodies with dilutions in TBST and 3 % BSA noted in Table 4 were treated overnight (4°C). An exception was made for anti-GAPDH. In this case treatment for 2 h at RT and dilution in TBST and 5 % powdered milk is sufficient.

Next PVDF was washed three times in TBST/BSA each for 10 min and tagged for 1 h with horseradish peroxidase-conjugated secondary antibodies (rabbit or mouse) diluted in TBST

with 3 % BSA (for GAPDH dilution in 5 % powdered milk is sufficient). For chemiluminescent detection membrane was treated with ECL WB substrate or SuperSignal WestDura Substrate (both Thermo Scientific Pierce). For quantification gel documentation software from VWR was used including normalization to the house keeping protein Gapdh.

Table 4. Protocol for immunodetection of used antibodies

Primary Antibodies	Catalog No.	Host Species	Company	Dilution
anti-NOS1AP, monoclonal	ab190686	rabbit/IgG	abcam	1 : 750
anti-GAPDH, monoclonal	MA116757	mouse/IgG	Thermo Fisher	1 : 2000
anti-NOS1, monoclonal	37-2800	mouse/IgG	Thermo Fisher	1 : 1000
anti-LTCC, monoclonal	MA527717	mouse/IgG	Thermo Fisher	1 : 2000
anti-ProBNP, monoclonal	MBS2090589	mouse/IgG	MyBioSource	1 : 1000
anti-PMCA4b, monoclonal	sc-20027	mouse/IgG	Santa Cruz	1 : 300
anit-SERCA2a, monoclonal	sc-376235	rabbit/IgG	Santa Cruz	1 : 500
Secondary Antibodies				
anti-rabbit, HRP, superclonal	A27036	goat/ IgG	Thermo Fisher	1 : 2000
anti-mouse, HRP, polyclonal	NXA931	sheep/ IgG	GE Healthcare	1 : 2000

Co-Immunoprecipitation

Co-localization analyses were performed by using the immunoprecipitation starter pack consisting of protein A/G sepharose (GE Healthcare) and recommended user instructions. In short; 70 µl protein A/G sepharose mix was incubated for 2 h with 3 µl monoclonal anti-NOS1AP (ab190686) on a rotating mixer, ~60 µg samples were added and mixed overnight at 4°C. Controls (beads) containing no antibody and the sample were added as mentioned above. Pellet was washed twice with the same lysis buffer used for protein extraction by centrifugation at 12 000 x g for 30 s between each wash. The final pellet was mixed with Laemmli sample buffer and heated for 4 min at 95°C. Supernatant was loaded on SDS-PAGE and transferred to a PVDF membrane the same way as described in this Section 2.4.2. *Western Blot and Immunodetection,* but immunodetection was conducted with anti-SERCA2a respective anti-PMCA4b.

2.4.3. Immunofluorescent Staining of Ventricular Myocytes

For immunocytochemistry isolated ventricular cardiomyocytes were fixed (4 % formaldehyde) on laminin coated coverslips and stained following a protocol including permeabilization with 0.1 % Triton X-100, blocking for 1 h in 1 % goat serum and 0.1 % BSA in PBS and incubation with anti-NOS1AP (ab190686, 1 : 300 dilution) and anti-LTCC (MA527717, 1 : 500 dilution) antibodies

in the same blocking solution overnight (4°C) in a humidity chamber. The following day started with three times washing and incubation for 1 h with secondary goat anti-rabbit (#F-2765, Thermo Fisher, dilution 1:500) respective goat anti-mouse (#A10521, Thermo Fisher, dilution 1:250) FITC or Cyanine3 conjugate antibodies followed by washing and DAPI (0.5 µg/ml) staining. Finally, immunofluorescent detection with the KEYENCE BZ-X800 Fluorescence Microscope was performed. For cyanine3 TRITC filters (excitation max 554, emission max 568) and for FITC special filter for excitation max 490 and emission max 525 were used.

2.4.4. Hematoxylin-Eosin and Fibrosis Staining of Heart Cross Section

The staining was kindly performed in collaboration with the Max Delbrück Center for Molecular Medicine in the Helmholtz Association (MDC). Hearts were halved and the top was fixed (4 % formaldehyde) overnight followed by paraffin-immersion using the tissue processor STP120 (Thermo Scientific, in Table 5 the protocol is depicted) with basket agitation function level 1. Afterwards tissue was transferred in special paraffin boxes for embedding and cooled paraffin wax blocks were sliced with a rotary microtome HM355S (Fisher Scientific) or CUT 6062 (SLEE) with a section transfer system in 4 µm sections and mounted on slides.

Table 5. Protocol for paraffin-immersion

Step	Bath reagent	Duration (minutes)
Dehydration	70 % Ethanol	30
	70 % Ethanol	30
	80 % Ethanol	30
	80 % Ethanol	30
	96 % Ethanol	60
	96 % Ethanol	60
	Isopropanol	60
	Isopropanol	60
Transparentizing	Xylene	90
	Xylene	90
Immersion	Paraffin Wax	90
	Paraffin Wax	120

Before staining the slides were deparaffinized and rehydrated as follows; three times in xylene, three times in 96 % ethanol, 90 % ethanol, 80 % ethanol, 70 % ethanol, 50 % ethanol, 30 % ethanol (each step for 5 min) and finally followed by another wash step for 10 min in water. For hematoxylin-eosin (H&E) staining slides were incubated for 6 min in Hämatoxylin Solution Gill No.1 (Fa. Sigma Aldrich), rinsed two times in tape water followed by incubation for 30 seconds in Eosin Y solution, alcoholic (Fa. Sigma Aldrich). When staining was completed, the dehydration was performed (each step 3 min): 80 % ethanol, 90 % ethanol, 100 % ethanol, isopropanol and finally for 30 min in xylene. Slides were mounted using Eukitt Quick-hardening mounting medium (Fa. Sigma Aldrich). Fibrosis staining was conducted using picro-sirius Red Solution (Fa. Sigma Aldrich) and incubating for 70 min in the dark followed by quick rinsing in 0.5 % acetic acid in tape water, quick dehydration in 100 % ethanol and 20 min incubation in xylene. Images were taken with the Aperio AT2 176 brightfield digital scanner (Leica Biosystems, Nussloch, Germany). Measurements of dimensions were conducted with the supplied Aperio Image Scope Software and the ruler tool.

2.4.5. ECG Measurements

Electrocardiography measurements (LabChart v8.1.16., AD Instruments) were recorded after light sedation of mice with isoflurane CP (1 ml/ml, cp pharma) inhalant anesthesia with a dose of 2 - 3 % isoflurane. Recordings in lead I configuration were studied for 1 – 5 min using needle electrodes and Bio Amp modules with a PowerLab 4/26 (ADInstruments) and analyzed with the corresponding LabChart software using a range of 500 µV and low pass (100 Hz) / high pass (300 Hz) filters. The ECG analysis tool excluded invalid beats automatically and gave the opportunity of graphical representation. For statistical evaluation SPSS statistics (IBM) was utilized.

To monitor spontaneously occurring arrhythmias or cardiac events a mouse telemetry was conducted in accordance to a standard protocol. A transmitter was transplanted dorsal with a postsurgical recovery phase of 7 days. Cardiac potential changes were recorded for 24 h in special mouse telemetry cages allowing free movements of animals. Signals were sent to a receiver located on the bottom of cages for subsequent interpretation (Spiranec et al., 2018). The measurements were conducted in cooperation with Professor Kai Schuh at the University of Wuerzburg.

2.5. Whole-Cell Patch-Clamp Measurements in freshly isolated Ventricular Myocytes

The measurements were kindly done in collaboration (Professor Lars Maier) with the University Hospital Regensburg. Freshly isolated ventricular myocytes were plated on laminin (1-2 mg/ml, Sigma-Aldrich) coated perfusion chambers and allowed to attach for 15 min. Cells were washed twice with patch-clamp bath solution (see Table 6 for ingredients) to discard dead cells and artefacts. For measurements (performed at RT) the perfusion chamber was inserted to a special object table adapter of an inverted microscope (Zeiss Axio Observer) with integrated DCS-120 confocal scanning FLIM system (B&H) for lifetime imaging surrounded by a faraday cage (Figure 8).

Figure 8

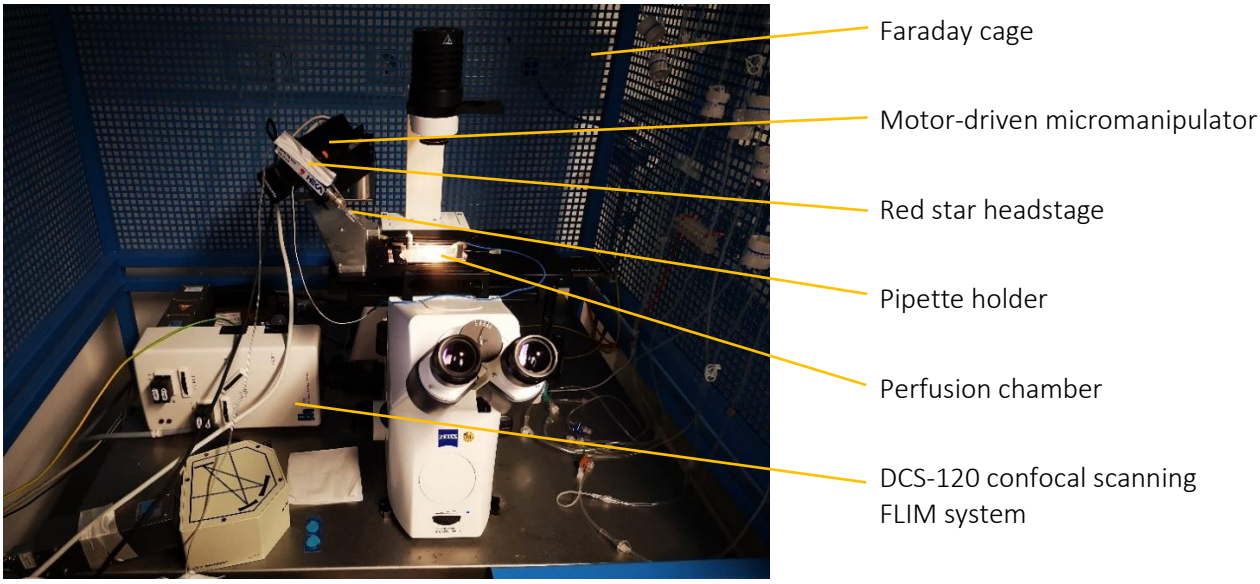

Legend to Figure 8. Patch-clamp equipment at the University Hospital Regensburg with (labeled) elements

Currents flow in a complete circuit. Therefore, one electrode was immersed to the extracellular bath solution and the other electrode is located in the middle of the patch pipette enveloped with pipette solution containing 122 K-Aspartic Acid, 10 NaCl, 8 KCl, 1 MgCl2, 5 Mg-ATP, 0.3 Li-GTP and 10 HEPES (mM), pH 7.2 with KOH. Patch pipettes (borosilicate glass capillaries, world precision instruments) were freshly pulled and heat polished using the DMZ-Universal Puller (Zeitz Puller GmbH) until a recommended resistance of the pipette of 2-4 MΩ was obtained. The pipette solution was filled freshly (MicroFil, world precision instruments) before each single trial. It was crucial not to damage the cells by patching, so for careful navigation the pipette holder was coated on a motor-driven micromanipulator (scientifica).

The first settings were done visually using an ocular and navigating the pipette near the selected cell. For fine-tuning the transformed digital signals were monitored on the PC using a pulse protocol (Figure 9). To be able to see such signals an A/D converter (Dalanco Spry Model 250, Dalanco,Rochester, USA) is integrated to the patch-clamp apparatus. Furthermore, it is equipped with Bessel filters (2.9 and 10 kHz) and an EPC10 amplifier with a red star headstage coated to the pipette holder (HEKA Elektronik) to reduce background noises.

Patching cells is easier by carefully lowering pressure in the patch pipette, resulting in closer distance to the cell membrane until the gigaseal (electrical resistance ≥ 1 GΩ) is reached. Figure 9 gives an example for obtained digital signals of a seal or a leak pulse.

Figure 9

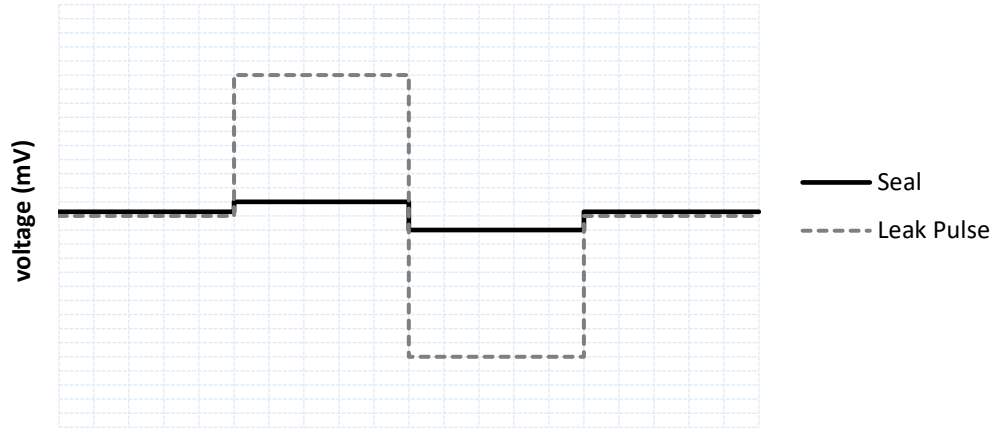

Legend to Figure 9. Example for a pulse protocol. Reaching the gigaseal (≥ 1 GΩ) reduces the pulse amplitude to a straight line. High amplitude means a small electrical resistance between the patch pipette and the cell membrane standing for poor sealing

Modifications and recordings were made with the associated Patchmaster software and the obtained results were analyzed using Microsoft Excel, LabChart and GraphPad PRISM.

Once a gigaseal between the patch pipette and the cell membrane was obtained a negative pressure ruptures the membrane and the software changes to a whole-cell modus. For recordings, the cardiomyocytes had to be vital without depolarization abilities. The gigaseal provides a strong isolation between bath solution and pipette solution. Afterwards the action potential (AP) can commence in whole-cell current-clamp configuration, stimulated by square current pulses of 1-2 nA amplitude and 1-5 ms duration at a frequency of 1 Hz.

For a detailed description of patch-clamp equipment and recordings specialized literature is recommended (Numberger & Draghuhn, 1996; Sakmann & Neher, 2009).

Table 6. Ingredients for 10x stock of bath solution

Final concentration	Ingredients
140 mM	Sodium chloride NaCl (58.4 g/mol)
4 mM	Potassium chloride KCl (74.6 g/mol)
1 mM	Magnesium chloride $MgCl_2$ (95.21 g/mol)
5 mM	2-[4-(2-hydroxyethyl)piperazin-1-yl]ethanesulfonic acid HEPES (238.31 g/mol)
Ad deionized water, adjust pH to 7 with Sodium hydroxide (NaOH)	
For 1x solution dilute 10x stock solution and ad freshly:	
10 mM	Glucose (180.16 g/mol)
1 mM	Calcium Chloride $CaCl_2$ (use 100 mM $CaCl_2$ solution)
Ad deionized water, adjust pH to 7.4 with Sodium hydroxide (NaOH)	

3. Results

3.1. Genotyping of the Nos1ap Double Transgenic Mice

Transgenic Nos1ap^{+}/αMHC-tTA^{-} mice were revitalized successful by the transgenic core facility (TCF) of the MDC, followed by mating with FVB.Cg-Tg(Myh6-tTA)6Smbf/J mice (The Jackson Laboratory) to obtain DT mice.

All mice were genotyped a second time after sacrificing to check the correct genotype for group classification. PCR products mixed with GelRed (Biotium) and loading dye were loaded on a 2 % agarose gel for electrophoresis and for sizing a 50 bp DNA ladder (VWR Chemicals) was used. The product of Nos1ap^{+} mice has a size of 201 bp and the tTA amplicons (primers of the Jackson Laboratory) for genotyping transgenic αMHC-tTA^{-} mice results in 200 bp (Tctr) and an additional 450 bp (tTA) band depicted αMHC-tTA^{+} animals. Lane 1 to 5 shows examples for genotyping by PCR of Nos1ap and lane 6 to 10 of tTA primer combinations. Figure 10 shows the correct size of PCR products for genotyping with detailed explanation of lanes 1 to 10.

Figure 10

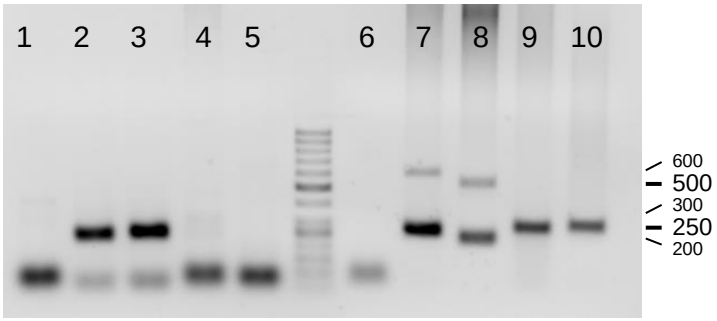

Legend to Figure 10. Electrophoresis of genotyping by PCR with ladder in the middle of the gel. No template control (lanes 1, 6), Nos1ap^{+} (lanes 2, 3), Nos1ap^{-} (lanes 4, 5), tTA^{+} (lanes 7, 8), tTA^{-} (lanes 9, 10)

3.2. Characterization of the Nos1ap Phenotype

The used FVB mice are distinguished by an albino phenotype. To take into account the physical, physiological and behavioral needs of the species *Mus musculus,* the room temperatures was adjusted to 23°C with a 12 h/12 h circadian rhythm. The mice live in small groups of 3 to 6 animals with nesting material with appropriate housing space and access to water / food *ad libitum* (Figure 11). Cages were changed frequently and score sheets were used for routine monitoring of health.

Figure 11

Legend to Figure 11. Example for housing conditions of laboratory FVB mice used for this project

3.2.1. Confirmation of Heart-Specific Nos1ap Overexpression

Protein expression analysis was conducted to confirm the cardiac Nos1ap overexpression in DT mice following gene induction due to removal of doxycycline from diet (*Tet-off*). To determine protein concentration for the following SDS-PAGE a Bradford (Bradford MM, 1976) colorimetric assay was conducted as described in Section 2.4.2. Final quantification of Nos1ap was given in relation to the house keeping gene Gapdh. Equal amount of samples was also determined by SDS-PAGE with final Coomassie gel staining. In Figure 12 a Coomassie stained gel loaded with equal amount of different ventricle samples and also with samples from other tissues is given. The protein expression differs depending on the origin of the utilized sample material. For example, the myosin heavy chain (MHC, 223 kDa) protein expression is enhanced in ventricular cardiomyocytes compared to those in non-muscle cells (Figure 12).

Figure 12

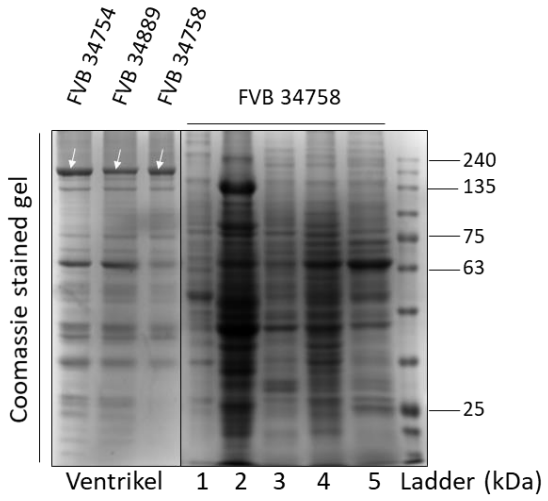

Legend to Figure 12. Coomassie gel staining of SDS-PAGE loaded with protein extracts of ventricular cardiomyocytes including mouse numbers, other tissue samples and ladder. Brain (1), liver (2), spleen (3), kidney (4), lung (5). Arrow: myosin heavy chain protein

In Figure 13A representative results of the immunodetection analysis with anti-NOS1AP (~56 kDa) and anti-GAPDH (~36 kDa) antibodies are depicted. As described in Chang et al. (2008) a short-form (~30 kDa) and a full-length (~56 kDa) isoform of Nos1ap is expressed in the heart. They found only interaction of the full-length Nos1ap isoform and Nos1. In our data the full-length (~56 kDa) isoform of Nos1ap is represented. Major expression of Nos1ap occurs in brain tissue used as a positive control for western blots. On the left side ventricular tissue of non-induced and on the right-side ventricular tissue of induced Nos1ap overexpressing mice were depicted in Figure 13A. For protein quantification a normalization to Gapdh was utilized. Statistical box plot analysis of the Nos1ap quantification is depicted in Figure 13B (n = 9). A 2.5-fold decrease of Nos1ap expression was observed in non-induced animals.

Figure 13

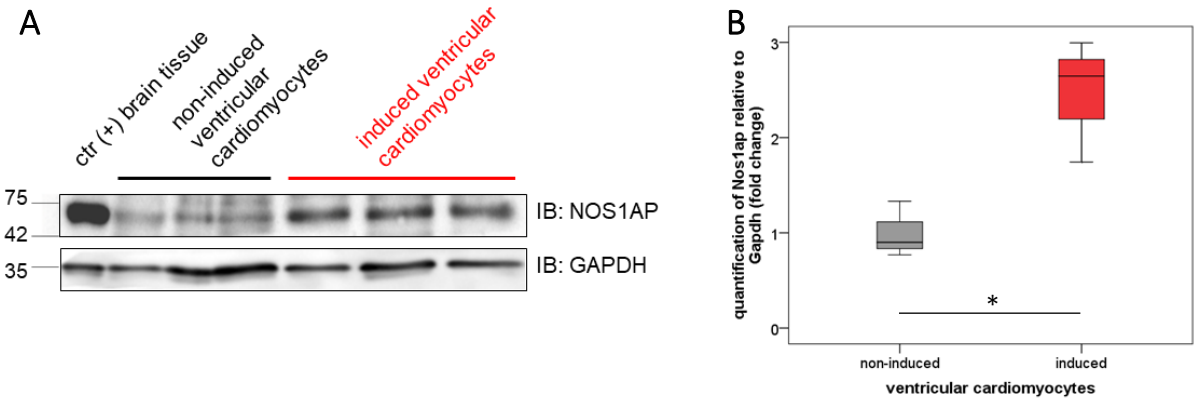

Legend to Figure 13. Representative protein expression analyses (A) of induced and non-induced heart-specific Nos1ap over-expression in transgenic mice with (B) statistical evaluation (n = 9, $p < 0.05$)

To confirm heart-specific overexpression of Nos1ap different tissues collected from mice ten days after induction, compared to controls, were analyzed (n = 3). We found no significant increase in Nos1ap expression in tissues other than the heart due to induction by changing mouse diet 10 days before sacrificing the animals (Figure 14).

Figure 14

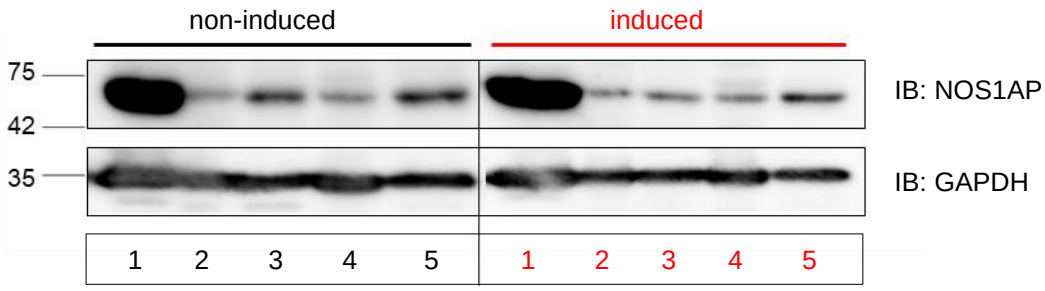

Legend to Figure 14. Representative Nos1ap immunoblotting of different tissues of mice with (induced) and without (non-induced) cardiac Nos1ap overexpression (n = 3). Brain tissue (1), liver tissue (2), spleen tissue (3), kidney tissue (4), lung tissue (5)

In preliminary investigations (Section 1.5.) interaction of Nos1ap with Nos1 and LTCC was detected. Following that assumption, we wanted to evaluate the influence on basic Nos1 expression depending on the amount of Nos1ap in cardiomyocytes (Figure 15). The murine Nos1 exhibited a band at about 160 kDa in a western blot. In a Pearson correlation analysis, we found no correlation (n = 5, coefficient = 0.207) between Nos1ap and Nos1 expression levels (Figure 15B). Figure 15C depicts in a box plot analysis a significant (n = 5, p = 0.01) difference between Nos1ap und no significant (n = 5, p > 0.05) difference between Nos1 expression in induced vs. non-induced mice.

Figure 15

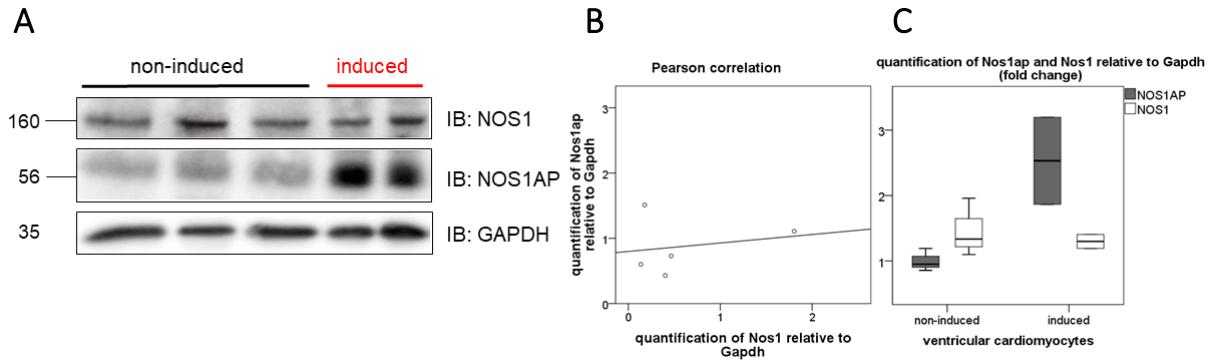

Legend to Figure 15. Representative western blots (A) and statistic evaluation by Pearson (B, coefficient=0.207, not significant) or by unpaired t-test (C) from Nos1ap overexpressing (induced) and normal (non-induced) ventricular cardiomyocytes (n = 5). Results of protein quantification were normalized to Gapdh

Furthermore, we confirmed the co-localization of Nos1ap and LTCC in immunofluorescence microscopy (Figure 16). Immunoreactive signals has been detected by antibodies in fixed adult cardiomyocytes incubated with anti-LTCC and anti-NOS1AP respective. Both protein staining's revealed signals distributed over whole cells and by merged overlay a broadly co-reactivity was confirmed.

Figure 16

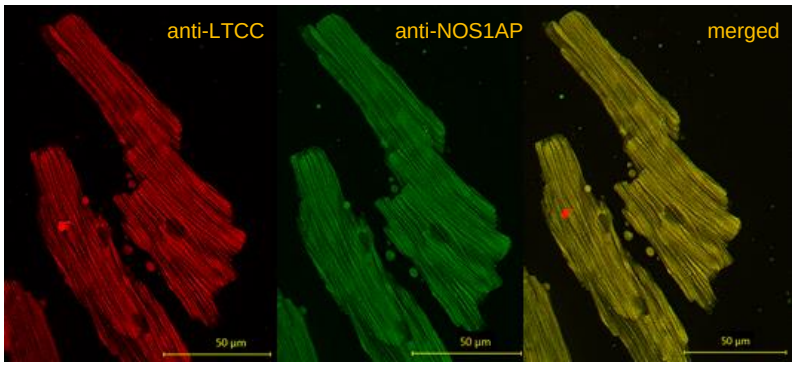

Legend to Figure 16. Immunofluorescence microscopy images made with the KEYENCE BZ-X800 Fluorescence Microscope. Nos1ap was coupled with FITC (green) and LTCC with Cyanine3 (red) conjugated antibodies and imaged by using special filters for excitation and subsequently emission detection. Merged images show co-localization of both proteins

3.2.1. Nos1ap Co-Immunoprecipitation Study with SERCA2a and PMCA4b Antibodies

Further investigations were performed to determine protein-protein interaction studies of Nos1ap. In preliminary data we have found that Nos1ap specifically co-localize with both, Nos1 and LTCC and co-reactivity was stronger in induced animals respectively (Figure 2). To further analyze the influence on other ion channels on cardiac calcium cycling we performed additional co-immunoprecipitation experiments. As mentioned at the beginning (Section 1.1.) SERCA mediates the re-uptake of calcium ions into the SR. In this regard, Burkard et al. (2007) have found a co-reactivity of Nos1 and the plasma membrane calcium ATPase (PMCA), a membrane structure which is responsible for pumping calcium from cytosol into the extracellular space. Own results showed no interaction with SERCA2a and PMCA4b (Figure 17). The isoform of SERCA2a is expressed in heart. The cardiac isoform 4b of PMCA was described as a negative regulator of Nos1 and that's why it seems to be of special interest for our project (Schuh et al., 2001). In Figure 17 immunoprecipitation of Nos1ap was conducted followed by immunoblotting with PMCA4b, SERCA2a and Nos1ap antibodies. The latter immunoblot with the Nos1ap antibody in the same experiment with SERCA2a and PMCA4b serves as positive control for immunoprecipitation procedure with agarose beads.

Figure 17

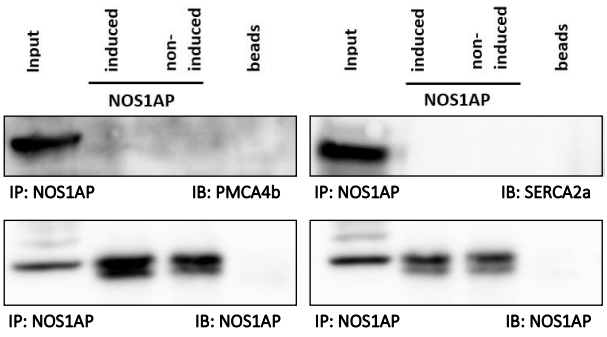

Legend to Figure 17. Co-immunoprecipitation of Nos1ap and immunoblotting with Nos1ap (positive control), PMCA4b (left) and SERCA2a (right) by using heart tissue extracts from mice with or without Nos1ap overexpression

3.2.2. Heart Histology and Surrogate Marker for Heart Failure

So far, the Nos1ap overexpression was confirmed in DT Nos1ap^{+}/αMHC-tTA^{+} mice compared to control mice and we found no interaction with Nos1ap and other calcium channels than the LTCC. Basic Nos1 expression is unaffected by different Nos1ap levels in cardiomyocytes. For further characterization heart cross sections were conducted and in Figure 18 representative H&E staining's of heart tissue, taken of Nos1ap overexpressing and control mice, were imaged.

No morphologic changes in cell structures were observed between both groups. Find blue colored the nucleic acids in nuclei and pink colored unspecific protein staining's in cytoplasm.

Figure 18

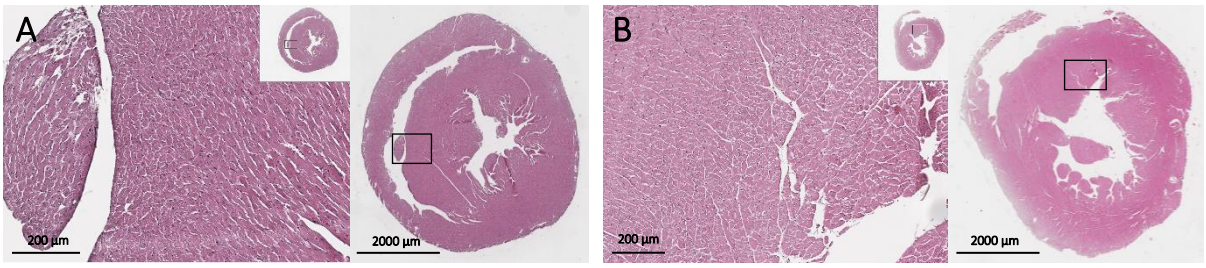

Legend to Figure 18. Representative H&E staining's of heart cross sections taken from non-induced (A) and induced (B) mice with corresponding photomicrographs of normal myocardial branching structure in both groups

For determination heart dimensions and fibrosis content different heart cross sections of the same mice as taken for H&E staining were utilized. Collagen fibers used as a marker for fibrosis and were stained by picro-sirius Red. Fibrosis were red- and muscle and cytoplasm yellow-colored under light microscopy. Figure 19 shows representative images and statistical evaluation (non-induced n = 8, induced n = 6). We found no indications of structural heart diseases as left ventricular wall thickness (2.01 ± 0.33 mm vs. 1.87 ± 0.23 mm in induced mice). Heart diameter cross sections (5.69 ± 0.25 mm vs. 5.45 ± 0.34 mm in induced mice) and fibrosis content (1.3 ± 0.42 % vs. 0.85 ± 0.93 % in induced mice) were also not altered significantly after three month of induction the Nos1ap overexpression compared to non-induced controls.

Figure 19

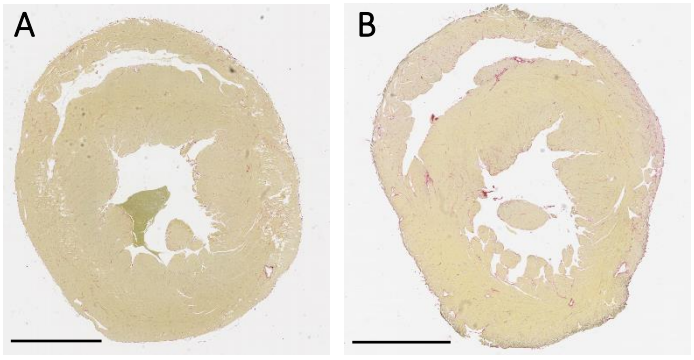

C	non-induced	induced	p-value
left ventricular wall thickness	2.01 ± 0.33 mm	1.87 ± 0.23 mm	0.46
diameter heart cross section	5.69 ± 0.25 mm	5.45 ± 0.34 mm	0.16
fibrosis content	1.3 ± 0.42 %	0.85 ± 0.93 %	0.26

Legend to Figure 19. Representative picro-sirius Red stain of heart cross sections taken from non-induced (A) and induced (B) mice [bar = 2000 µm] with statistical evaluation (C) given in averaged values (± SEM) for left ventricular wall thickness, diameter of heart cross section and collagen content as maker for fibrosis (non-induced n = 8, induced n = 6)

In Figure 20 more images of the heart fibrosis staining of Nos1ap overexpressing mice (n=6) and representative staining's of controls (n =6) were depicted.

Figure 20

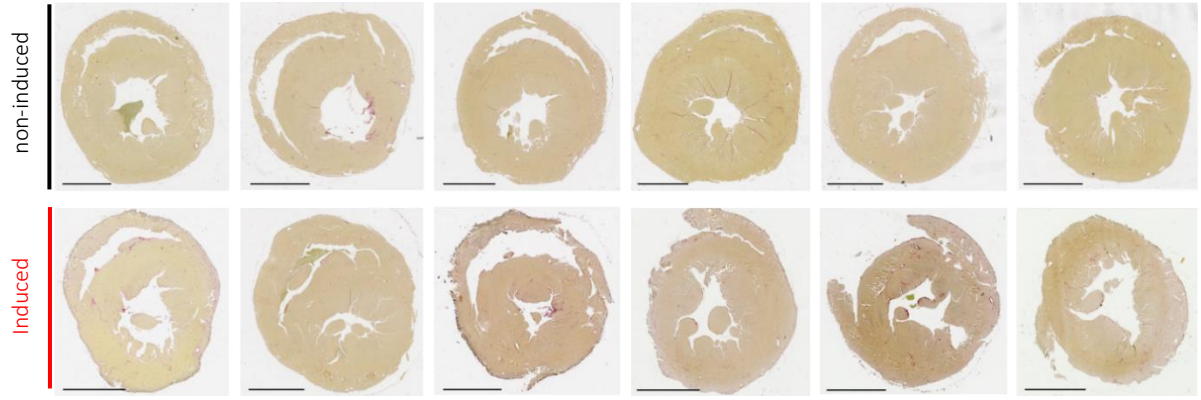

Legend to Figure 20. Picro-sirius Red stain of heart cross sections (n = 6) taken from non-induced and induced mice with no indication for structural heart diseases due to Nos1ap overexpression [bar = 2000 µm]

In addition, brain natriuretic peptide (BNP) has been used as a marker for heart dysfunction. Physiologically, the pro-hormone BNP is cleaved in the active BNP and the inactive N-terminal pro (NT-pro) BNP form. NT-proBNP is more stable than BNP and is also a marker for cardiac function (Dronavalli et al., 2010). Quantitative NT-proBNP measurements gave no signs of heart failure due to induction of the transgenic phenotype (1.16 ± 0.8 in non-induced to 1.25 ± 0.85 in Nos1ap overexpressing mice, n = 6, p = 0.25, Figure 21).

Figure 21

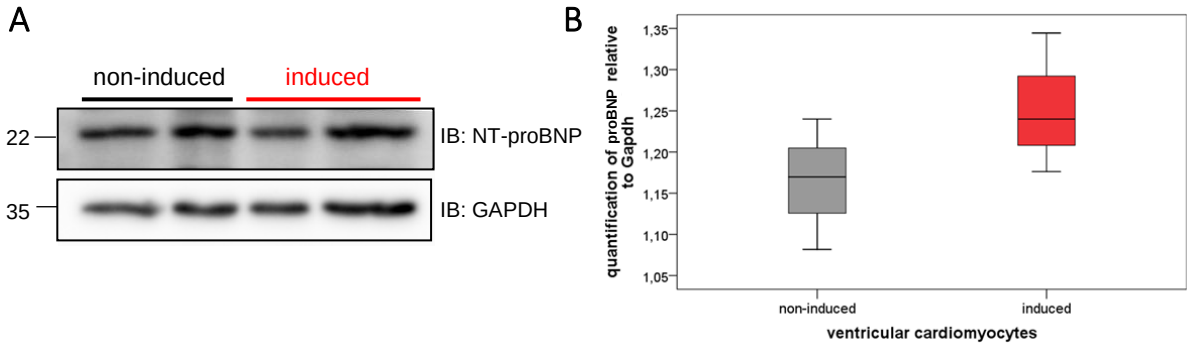

Legend to Figure 21. Representative quantification of NT-proBNP in a western blot (A) with statistical evaluation (B), values were normalized to Gapdh (n = 6, p = 0.25)

3.2.3. Heart Weight Normalized by Body Weight

Further characterization of heart weight to body weight was determined in the mice ten days (Table 7, Time point 1) or 100 days (Table 7, Time point 2) after inducing the transgenic phenotype. All mice were nearly in the same age of 15.7 ± 3.8 weeks (non-induced) respective

14.5 ± 3.2 weeks (induced) at time point 1 and 32.4 ± 5.9 weeks (non-induced) respective 26.1 ± 5.6 weeks (induced) at time point 2. Statistical analysis was performed with SPSS and the unpaired t-test and depicted in Figure 22 using a box plot analysis.

Table 7. Characterization of mice 10 days (Time point 1) and 100 days (Time point 2) after (non) induction the Nos1ap overexpression. Age and weight of body, heart, brain, liver, spleen, kidney, lung is given with standard deviation (n = 6 to 11)

	Time point 1		Time point 2	
Condition	non-induced	induced	non-induced	induced
Age in Weeks	15.7 ± 3.8	14.5 ± 3.2	32.4 ± 5.9	26.1 ± 5.6
Body Weight (BW)	29 ± 3.9 g	26.7 ± 4.1 g	41.1 ± 5.0 g	34.1 ± 4.1 g
Heart Weight (HW)	0.166 ± 0.02 g	0.193 ± 0.06 g	0.182 ± 0.03 g	0.190 ± 0.02 g
Brain Weight	0.408 ± 0.11 g	0.349 ± 0.09 g	0.438 ± 0.03 g	0.482 ± 0.02 g
Liver Weight	1.700 ± 0.22 g	1,444 ± 0.28 g	1.675 ± 0.21 g	1.704 ± 0.22 g
Spleen Weight	0.133 ± 0.04 g	0.207 ± 0.28 g	0.116 ± 0.02 g	0.130 ± 0.01 g
Kidney Weight	0.516 ± 0.10 g	0.426 ± 0.11 g	0.498 ± 0.11 g	0.424 ± 0.123 g
Lung Weight	0.206 ± 0.07 g	0.153 ± 0.05 g	0.174 ± 0.04 g	0.171 ± 0.017 g
HW / BW Ratio	0.0058 ± 0.008[#]	0.0073 ± 0.003	0.0045 ± 0.0006[#]*	0.0056 ± 0.0003*
Sample Size	n = 10	n = 10	n = 11	n = 6

[#]*$p < 0.05$

We found significant differences in Heart Weight / Body Weight (HW / BW) Ratio between both time points for non-induced but not for induced mice. Furthermore, HW / BW Ratio was significant higher in induced than in non-induced animals at time point 2. That stands here for nearly the same HW (0.182 ± 0.03 g vs. 0.190 ± 0.02 g in induced animals) and higher BW (41.1 ± 5.0 g vs. 34.1 ± 4.1 g in induced animals) in non-induced animals. As we found no differences in heart dimensions and fibrosis content using structural heart analyses between induced and non-induced mice, we conclude that the influence of different chows leading to a differential HW / BW Ratio, more than abnormal structural cardiac development like hypertrophy or other diseases.

Figure 22

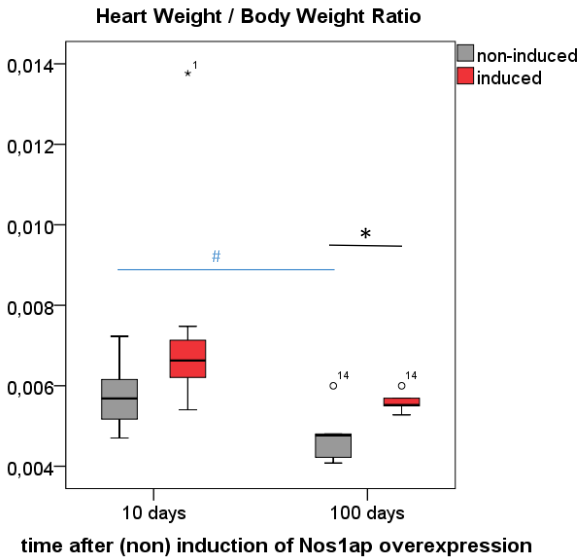

Legend to Figure 22. Box plot analysis excluding the outliers of HW / BW Ratio in mice with cardiac Nos1ap overexpression compared to controls at different time points after induction the transgene (for 10 or 100 days) with statistical evaluation #*p < 0.05

3.2.4. Arrhythmias and Shortening of QT due to Nos1ap Overexpression and long-term Experiments

The influence of cardiac overexpression of Nos1ap in whole organism was studied by ECG recordings. ECG analyses were conducted under light sedation using the PowerLab 4/26 and Bio Amp modules (ADInstruments). In Figure 23 (A1/2 to C1/2) representative ECG measurements were depicted using the ECG analysis module of the LabChart software. Both experimental groups showed in A1/2 a normal basic sinus rhythm. For representation the QT interval a Waterfall Plot is selected in B1/2 and there was a clear decrease in QT intervals (20 ± 1.9 vs. 28 ± 4.6 ms, n = 6, $p < 0.05$) due to Nos1ap overexpression (Figure 23 B2) compared to non-induced animals (Figure 23 B1). Same results were depicted in Figure 23 C1/2 with a Beat Averaging View including the QRS start and end of the t-wave for calculation of the QT interval in the ECG. As mentioned, in mice there is no need for a correction by heart rate, as Roussel et al. (2016, *Sci Rep*) found only weak relationship between the heart rate and the QT interval.

Figure 23

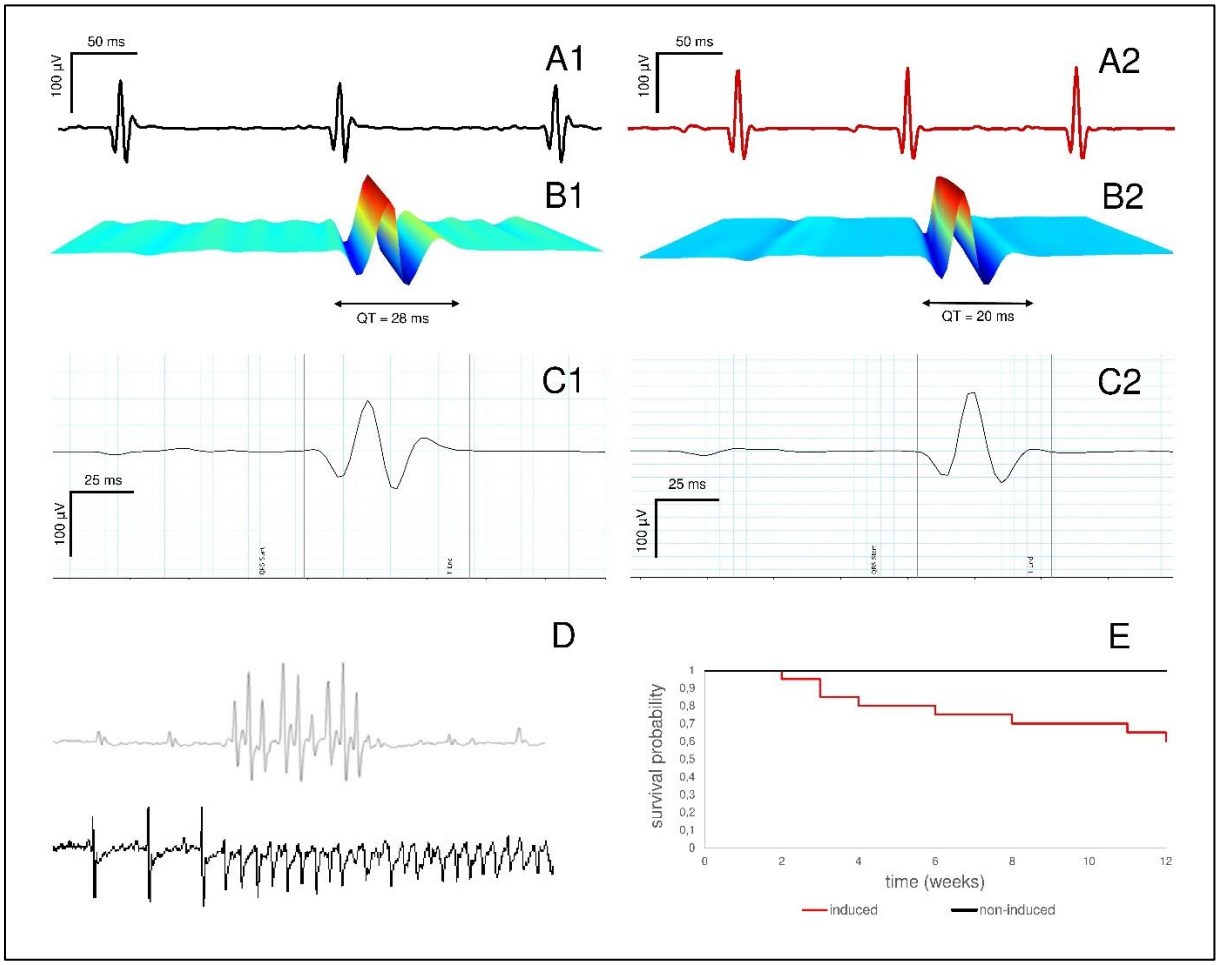

Legend to Figure 23. Electrocardiography in mice with (A/B/C2) / without (A/B/C1) cardiac Nos1ap overexpression showed significant decrease of QT intervals (B1/2, C1/2, 52 ± 1.8 vs. 63 ± 2.6 ms, $p < 0.05$) due to Nos1ap overexpression. (D) Mouse telemetry of induced mice resulted in ventricular tachycardia or ventricular fibrillation and in long-term experiments we found a reduced survival rate (E) in mice with Nos1ap overexpression compared to controls (n = 20)

No significant changes were observed in heart rate (481 ± 12 vs. 474 ± 11 beats/min, $p > 0.05$) and in the QRS duration (16 ± 1 vs. 17 ± 1 ms, n = 6, $p > 0.05$) in Nos1ap overexpressing compared to non-induced animals. To determine *in vivo* electrophysiological features for a longer period of time, mouse telemetry was conducted for 24 h and cardiac events were recorded. ECGs of non-induced animals showed a sinus rhythm, while Nos1ap overexpressing mice showed ventricular tachycardia or ventricular fibrillation (Figure 23D). The survival rate after 3 months of induction of Nos1ap overexpression was significantly reduced (60 % after 12 weeks vs. 100 % in non-induced mice) as demonstrated in Figure 23E. There were no behavioral or nutritional abnormalities before spontaneous death of the induced animals, indicating a relevance of spontaneous occurring arrhythmia.

The feeding is responsible for induction the Nos1ap overexpression (*Tet-off*), so by special diet the doxycycline binds to the tetracycline-controlled transactivator protein (tTA) leading to repression of the tetracycline-responsive element (TRE). In that case overexpression of Nos1ap is decreased. The QT alterations subsided upon re-administration of doxycycline (Figure 24).

Figure 24

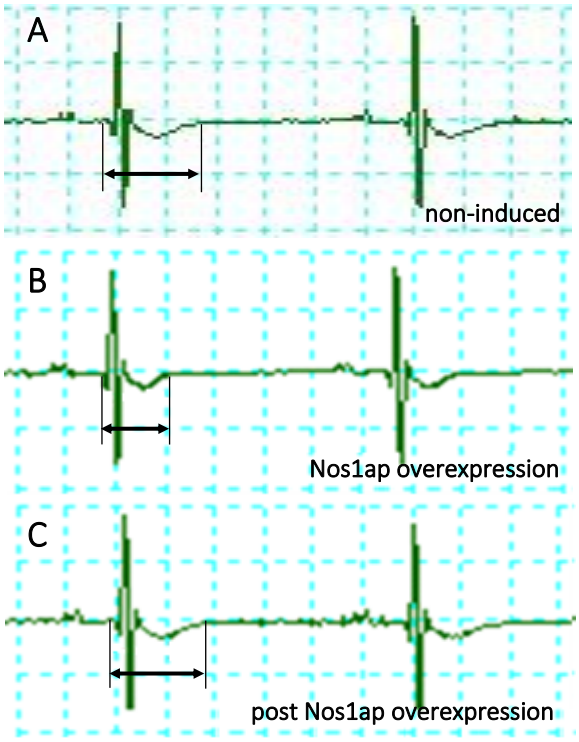

Legend to Figure 24. Representative ECG traces in non-induced (A), induced (B) and post-induced (C) mice. QT intervals were significantly reduced in induced vs. non-induced animals

3.3. Action Potential Duration Recordings in isolated Ventricular Myocytes

We found a clear decrease in QT intervals due to Nos1ap overexpression and a interaction of Nos1ap with Nos1 and LTCC. In further studies the action potential duration at 90 % of repolarization (APD_{90}) were elicited by current pulses of 1-2 nA amplitude and 1-5 ms duration at a frequency of 1 Hz by ruptured-patch whole-cell current clamp measurements. The APD_{90} in induced transgenic Nos1ap overexpressing mice was significant reduced compared to controls (44.6 ± 15.5 vs. 82.9 ± 43.7 ms). Figure 25A gives a correlation analysis of cardiac Nos1ap protein expression in different individuals and corresponding APD_{90} measurement. Action potentials were decreased in ventricular cardiomyocytes with higher Nos1ap protein expression (r^2 = 0.42). Altered APD_{90} values due to enhanced Nos1ap expression did not lead to significant changes in resting membrane potential or action potential amplitude (Figure 25B).

Figure 25

A

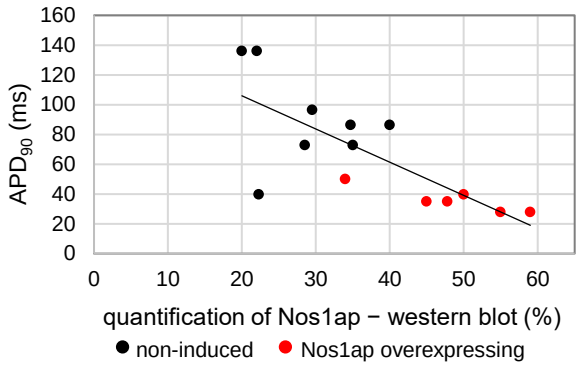

B

	non-induced	*induced*	*p-value*
resting potential (mV)	-65.3 ± 4.4	-65.1 ± 6.0	0.232
APA (mV)	92.8 ± 10.1	92.8 ± 6.0	0.997
APD90 (ms)	82.9 ± 43.7	44.6 ± 15.5	0.047

Legend to Figure 25. Correlation analysis of action potential duration at 90 % of repolarization (APD_{90}) recordings and Nos1ap protein expression pattern of cardiomyocytes from different transgenic FVB mice (A) and statistical evaluation in a table (B) with statistical evaluation using t-test. APA: Action potential amplitude (n = 6 induced, n = 8 non-induced)

Together with our previous data of a reduced promoter activity of the SNP rs16847548 located upstream of the Nos1ap gene and results of this investigations we conclude that there is a relevance of altered Nos1ap protein expression on QT interval duration. As the SNP rs16847548 was associated with QT prolonging effects in humans and overexpression of Nos1ap resulted in a reduction of the QT interval in our transgenic mouse model the presumed mechanism is depicted in Figure 26. Due to our confirmation of co-localization of Nos1ap with LTCC and Nos1 and further results in cell culture experiments (Chang et al., 2008) Nos1ap mediates the inhibition of LTCC due to enhanced S-nitrosylation of the channel together with APD_{90} shortening in cardiomyocytes of induced Nos1ap overexpressing animals (Figure 26) and that influence subsequently the QT interval.

Figure 26

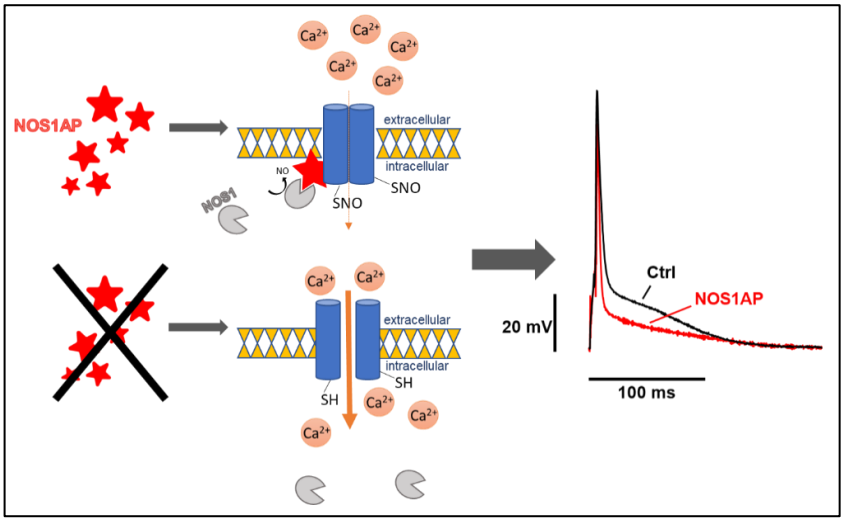

Legend to Figure 26. Graphical abstract of postulated mechanism of changed Nos1ap expression on LTCC with influence on action potential in ventricular myocytes. Traces of action potentials measured by patch-clamp in ventricular myocytes with Nos1ap overexpression (red) compared to controls (black)

4. Discussion

In more than 20 % of patients with the clinical diagnosis of an LQTS and in 80 % of patients with a SQTS diagnosis genotyping is negative (Garcia-Elias & Benito, 2018; Tester & Ackerman, 2014).

At the same time numerous genome-wide association studies (Kolder et al., 2015; Tomas et al., 2010; Zang et al., 2019; Zhang et al., 2017) showed polymorphisms in the *NOS1AP* gene that are correlated to QTc interval variations on the ECG. We hypothesized that NOS1AP acts as modulator of ion channel function, specifically of the L-type calcium channel (LTCC), to regulate action potential duration and the QT interval duration. Following this hypothesis our investigations were focused on the functional mechanism of Nos1ap regulating the QT interval by using a conditional transgenic overexpression mouse model.

Our results in summary: we performed a broad characterization of the transgenic Nos1ap overexpressing mouse model and found co-localization of Nos1ap with Nos1, LTCC and inhibition of $I_{Ca\text{-}L}$ by Nos1ap overexpression. Survival rate was significantly reduced three months after induction of the transgenic overexpression by sudden cardiac death (SCD). We found no signs for structural heart disease, but a clear decrease of the QT interval in the ECG and ventricular tachycardia in the holter ECG. Measurements using freshly isolated cardiomyocytes revealed an inverse correlation between the Nos1ap level obtained by western blot analyses and the APD_{90} values obtained by whole-cell patch-clamp technology.

4.1. Genotypes of QT interval Variations and the Influence of Nos1ap on cardiac Repolarization

QT interval prolongation is caused by delayed repolarization of the action potentials (APs) in ventricular cardiomyocytes (Tester & Ackerman, 2014). The AP depends on different ionic currents during the specific phases of de- and repolarization (Section 1.2. and Figure 1). The AP starts with a membrane depolarization due to fast sodium inward currents causing the negative resting membrane potential to be changed to a positive charge for a short period of time, until outward potassium channels are activated (and sodium inward currents are inactivated simultaneously) for repolarization and setting of the resting membrane potential again. Due to the slow calcium inward currents of the LTCC $I_{Ca\text{-}L}$ the repolarization is slowed down and a plateau phase is reached as positive charged calcium ions enter the cardiomyocytes. The inhibition of LTCCs leads to less calcium influx and subsequent shortening of the plateau phase

of the AP and a faster membrane repolarization (Figure 26) resulting in shortening of the QT interval in the ECG.

As mentioned above, there are different ion channels (mainly sodium, potassium and calcium) involved to shape the cardiac AP and hence it is not surprising that there are several susceptibility genes for *long* or *short* QT syndromes. Variants in *KCNQ1, KCNH2, SCN5A* (coding for ion channel α subunits) are mainly clinically relevant and were associated with LQTS type 1 to 3. The *long* and *short* QTS-susceptibility genes are summarized in Table 8 (Mazzanti et al., 2014; Tester & Ackerman, 2014).

Table 8. Identified genes harboring pathogenic mutations associated with QT interval variations adapted to Mazzanti et al. (2014) and Tester & Ackerman (2014)

Short QT Syndrome		*Long* QT Syndrome	
GENE	PROTEIN	GENE	PROTEIN
KCNJ2	I_{K1} potassium channel (Kir2.1)	*KCNQ1* (LQT1)	I_{Ks} potassium channel α subunit
KCNH2	I_{Kr} potassium channel α subunit	*KCNH2* (LQT2)	I_{Kr} potassium channel α subunit
		SCN5A (LQT3)	sodium channel α subunit ($Na_V1.5$)
KCNQ1	I_{Ks} potassium channel α subunit	*AKAP9*	Yotiao
CACNA1C	I_{Ca-L} L-type calcium channel ($Ca_V1.2$)	*CACNA1C*	I_{Ca-L} L-type calcium channel ($Ca_V1.2$)
		CALM1	Calmodulin
		CALM2	Calmodulin
		CAV3	Caveolin-3
		KCNE1	potassium channel beta subunit ($K_V7.1$)
		KCNE2	potassium channel beta subunit ($K_V7.1$)
		KCNJ5	Potassium inwardly-rectifying channel Kir3.4
		SCN4B	Sodium channel beta 4 subunit
		SNTA1	Syntrophin α1
		ANK2	Ankyrin B
		KCNJ2	I_{K1} potassium channel (Kir2.1)

Here, we investigated the relevance of Nos1ap, the adapter protein of Nos1, on cardiac electrophysiology, as it is associated with QT interval variations in humans (Kolder et al., 2015; Tomas et al., 2010; Zhang et al., 2017). As a main finding we saw shortening of the QT interval due to cardiac overexpression of Nos1ap in mice. The function of Nos1ap regarding interaction

with Nos1 and related Nos1-NO signaling pathways were studied previously in HEK293 cells and in guinea pig ventricular myocytes (Chang et al., 2008). The authors found an up-regulation of Nos1-NO signaling and an increase of LTCC nitrosylation in transfected Nos1ap overexpressing cells. Furthermore, they demonstrated Nos1ap dependent alteration of cardiac repolarization. In our project we extended the experiments from single cell level to whole animal physiology and investigated the impact of Nos1ap in a transgenic mouse model, to study the ECG phenotype and heart histology.

4.2. Cardiac Function and Targeting of Nos1 via its PDZ Binding Domain as Explanation for the Relevance of subcellular Localization in various Diseases

All three NOS isoforms (NOS1, NOS2 and NOS3, see also Section 1.4.) are expressed in heart tissue. The Nos1 isoform takes a prominent role on cardiac regulation due to its dynamic ability to change subcellular localization during different cardiac disease states (Strasen & Ritter, 2011). Other isoform-specific transgenic models demonstrated no differences in cardiac contractility; transgenic mice with a genetic deletion of *Nos3* showed no cardiac abnormalities under basal (physiological) conditions and *Nos2* also had no significant effect on basal cardiac function. In contrast Nos1 seemed to be involved in the regulation of the basal cardiac function (Sears et al., 2004). NOS1 is the only NOS isoform containing a PDZ binding domain beside the other co-factor binding sites of the enzyme (Figure 27). We focused here on the function of Nos1ap, acting as an adapter protein of Nos1 to $Ca_V1.2$ by using a transgenic mouse model with an inducible Nos1ap overexpression restricted to cardiomyocytes.

Figure 27

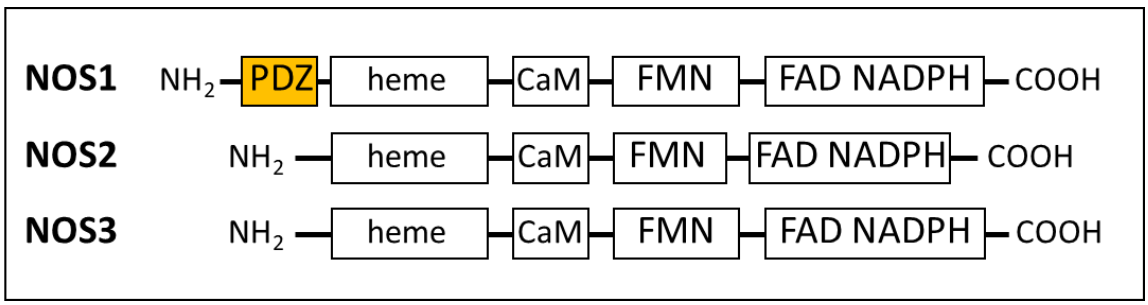

Legend to Figure 27. Simplified schematic drawing of NOS domain organization adapted to Campbell et al. (2014) depicting the PDZ binding domain (NOS1) and the co-factor binding sites for heme, calcium-calmodulin (CaM), flavin mononucleotide (FMN) and flavin adenine dinucleotide (FAD) / nicotinamide adenine dinucleotide phosphate (NADPH)

Molecular partnering and therefore subcellular localization of Nos1 obviously occurs via PDZ domains.

Schuh et al. proved the interaction of NOS1 with PMCA4b via their PDZ domains in HEK293 cells, causing a downregulation of NOS1 activity by PMCA4b due to its calcium transporter function and adjustment of the local intracellular calcium. In this work increased protein expression of PMCA4b led to a reduction of intracellular calcium concentrations with consequently a decreased calcium-dependent NOS1 activity (Figure 28). In this case NOS1 activity was inhibited by PMCA4b due to intracellular calcium release (Schuh et al., 2001). We now wanted to confirm a regulator function of Nos1ap as it tethers Nos1 and co-localizes it to the LTCC which leads to increased S-nitrosylation subsequently influencing the open probability of the LTCC.

Figure 28

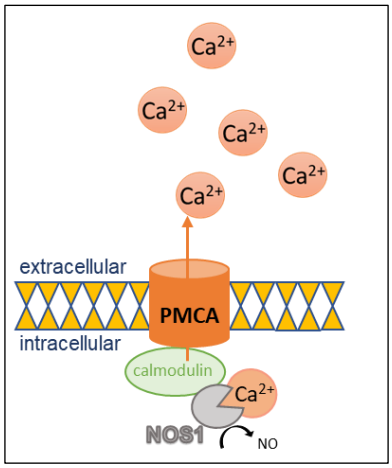

Legend to Figure 28. Model adapted to Schuh et al. (2001) depicting the interaction of the calcium/calmodulin-dependent NOS1 with the plasma membrane calcium / calmodulin-dependent calcium ATPase (PMCA). Outward calcium currents lead to a reduced NO production

The physical and functional interaction of PDZ domain-containing proteins was analyzed by Jaffrey et al. in three interesting studies. They found a regulatory impact of Nos1 on other proteins through PDZ-PDZ domain interactions (Jaffrey et al., 2002; Jaffrey et al., 2001; Jaffrey et al., 1998) as described hereafter. They confirmed the neuronal Capon (alias for Nos1ap)-mediated impact of Nos1 on synapsins (Jaffrey et al., 2002) and on the PSD95/NMDA receptor complexes (Jaffrey et al., 1998) due to mediated subcellular localization. Thus, the interaction of Nos1 and Nos1ap via the PDZ domain seems to have been confirmed, at least in the setting of neuronal cells. Zeng et al. reported another example of physical connection between neuronal CAPON (alias for NOS1AP) and NOS1 via the PDZ binding domain. It was hypothesized that schizophrenia may be triggered by abnormalities in glutamatergic transmission of NMDA receptors. Interaction of NOS1 with CAPON seems to disrupt the local NMDAR-mediated NO release leading to a schizophrenia pathogenesis (Zheng et al., 2005). Preliminary data from our

group (Section 1.5.) suggested in a similar way the co-localization of Nos1ap with Nos1 and $Ca_V1.2$ in cardiac tissue (Figure 2). Mu and colleagues were interested in the function of Nos1ap in the development of type 2 diabetes and insulin sensitivity as Nos1ap is also expressed in human and mouse hepatocytes. In general, impaired insulin sensitivity leads to a dysfunctional blood glucose metabolism with lower intracellular glucose uptake and higher liver lipid accumulation. They found that mice with a hepatic *Nos1ap* knockout showed impaired insulin sensitivity, but only those mice with a deletion of the full-length *Nos1ap* isoform containing the C-terminal PDZ binding domain. Overexpression of the full-length *Nos1ap* isoform abolished p38 MAPK phosphorylation leading to its inactivation and that mechanism has been reported to reduce insulin resistance in the liver. Overexpression of the N-terminal domain (without the PDZ binding site) of Nos1ap was not associated with a higher insulin sensitizing effect. (Mu et al., 2019).

Our genetic modification resulted in higher expression of the full-length isoform of Nos1ap, a protein of ~56 kDa (the protein (A1) and plasmid (A2) sequence are in the Appendix Section). We selected this approach because only the full-length isoform has been shown to co-localize with NOS1. Another short-length isoform (~30 kDa), that is likewise expressed in ventricular cardiomyocytes and contains also the C-terminal domain of NOS1AP, did not co-localize with NOS1 (Chang et al., 2008).

To the best of our knowledge this investigation is the first to describe a transgenic mouse model with a conditional overexpression of Nos1ap restricted to cardiomyozytes. There are some earlier studies using a transgenic Nos1 overexpressing mouse model for analysis of NO-mediated regulation in the heart. Previous investigations from our group, using a similar transgenic mouse model with a cardiac and inducible overexpression of Nos1, found a significant reduced ejection fraction and negative impact on LTCC due to Nos1 overexpression. Our results confirmed the impaired LTCC activity, as the AP was shortened in Nos1ap overexpressing animals and we speculated that is due to a lower inward calcium current in the plateau phase of the AP. Sun and colleagues found increased S-nitrosylation of the LTCC α1 subunit in female cardiomyocytes in combination with reduced $I_{Ca\text{-}L}$ currents. Nos blockade or genetic knockout of Nos1 in mice diminished the gender dependent decrease of $I_{Ca\text{-}L}$ in female mice (Sun et al., 2006). Jaffrey et al. pointed out that S-nitrosylation is a physiological signaling mechanism of Nos1 by using a S-nitrosylation assay. They utilized in initial tests brain lysates and by incubation with NO donor and doing the proteomic approach afterwards ~15 different

proteins, identified by mass fingerprinting method, were strongly S-nitrosylated. They identified here cytosolic and membrane-associated proteins for example GAPDH or ion channels subunits of NMDA and others. Further S-nitrosylation experiments were performed with brain extracts of $Nos1^{+/+}$ and $Nos1^{-/-}$ mice and subsequent immunoblotting of putative S-nitrosylated proteins. They could not find protein S-nitrosylation in mice with a targeted deletion of Nos1. Posttranslational modification of proteins like S-nitrosylation can cause either a gain or a loss of function depending on the target. Interestingly, they indicated that adapter proteins (such as Nos1ap) may provide access for Nos1 to other target proteins and determine S-nitrosylation (Jaffrey et al., 2001).

In a similar transgenic mouse model with an overexpression of Nos1 restricted to cardiomyocytes Burkard et al. found an interaction of Nos1 with SERCA2a. In control mice Nos1 was found near the SR but due to Nos1 overexpression they found an additional localization to the sarcolemma and also co-precipitation with $Ca_V1.2$. In Nos1 overexpressing animals $I_{Ca\text{-}L}$ was significantly diminished, intracellular calcium transients were impaired and the myocardial contractility was reduced. They assumed that the co-localization of Nos1 to $Ca_V1.2$ is important in that NO-dependent inhibition of LTCC is responsible for the negative inotropy (Burkard et al., 2007). We could not confirm an interaction of Nos1ap and SERCA2a (or PMCA4b) in this project and speculate here that Nos1ap had per se no effect on calcium cycling kinetics or affecting the contractility and consequently no influence on inotropy. However, conflicting results were provided by Beigi et al. who demonstrated interaction of Nos1ap and PMCA4b via the PDZ binding domain in PMCA4b as a novel translocation site in settings of cardiac injury post-myocardial infarction (Beigi et al., 2009). We might add, that Blackwell illustrates a varying calcium handling for EC coupling in mice respective humans. In humans, LTCC seems to have a higher impact and consequently NOS1AP might also have a more pronounced effect on EC coupling for myocardial contractility (Blackwell et al., 2022).

We found no evidence of structural heart disease in our transgenic mouse model assessed by fibrosis staining, histological analysis, NT-proBNP levels or HW/BW ratios. Typically, LQTS can lead to SCD also in young patients and is characterized by a normal cardiac morphology (Goldenberg et al., 2005).

Additionally, in mice structural cardiac diseases can be studied by analyzing the HW / BW Ratio. A relatively heavy heart compared to the body weight indicates for example heart failure or other cardiac diseases which are related with a changed heart volume. Our results rather

indicated here chow-dependent differential HW / BW Ratio due to three months of Nos1ap overexpression compared to controls. Consequently, heart weight normalized by tibial length ratio would have been a better fit than normalization to the bodyweight. This method was also used for quantification of cardiac hypertrophy in aging rats (Yin et al., 1982). To overcome chow-dependent divergences we also performed the histological heart analysis mentioned above.

As NOS1AP has no intrinsic enzymatic effect it earns its relevance by directing NOS1 to subcellular targets. Therefore, it is interesting to look at Nos1 overexpressing rodent models. Earlier studies of Burkard et al. found a cardioprotective effect in ischemia/reperfusion experiments in mice with conditional overexpression of Nos1. In Nos1 overexpressing animals there was an up-regulation of Nos1 in mitochondria (Burkard et al., 2010). It was proposed that Nos1 dependent protection against cell death is caused by reduced mitochondrial permeability. Increased mitochondrial membrane permeabilization was already described in the literature as a mechanism for cell death (Bock & Tait, 2020). In our transgenic mice we performed no ischemia/reperfusion experiments as we found no up-regulation of Nos1 protein levels and also a reduced survival rate in long-time experiments. In consequence a cardioprotective effect by mitochondrial inhibition or negative inotropy seemed not to be likely. Burkard et al. (2010) described the translocation mechanism of Nos1 via heat shock protein 90 (HSP90) into mitochondria.

A different transgenic mouse model with a heart-specific overexpression of Nos1 found delayed transition toward HF in response to pressure overload (transverse aortic constriction, TAC). In this rodent model, calcium reuptake into the SR was described, as major driver for developing HF. Calcium reuptake into the SR is mainly governed by SERCA activity which in turn is regulated by phospholamban (PLN), a known inhibitor of SERCA (Section 1.1.). Loyer et al. found increased calcium transients due to Nos1 overexpression in mice through modulation of PLN phosphorylation and related dissociation from SERCA which resulted in enhanced calcium reentry via SERCA. They found in contrast enhanced inward $I_{Ca\text{-}L}$ currents due to Nos1 overexpression and also increased cardiac contractility (Loyer et al., 2008).

Beigi et al. (2009) investigated the modulator function of Nos1ap (also known as CAPON) after myocardial infarction (MI). They observed translocation and accumulation of Nos1 at the plasma membrane after MI which protected cardiac myocytes from calcium overload. The postulated mechanism behind was nitrosylation and subsequent inhibition of the LTCC. In

contrast to post-MI wildtype (WT) mice, in Nos1 knockout mice, Nos1ap did not migrate to the plasma membrane known as typical consequence of MI as protection of cardiac injury due to calcium overload. Consistent with that observation our results confirmed the relevance of the interaction between Nos1ap, Nos1 and LTCC.

We did not observe an effect of cardiac overexpression of Nos1ap on the protein expression levels of Nos1. The subcellular localization of Nos1 governed by Nos1ap seemed to be more important than general increase in cytosolic NO levels as shown by the local effects of Nos1 on the LTCC. In general, the subcellular localization of Nos1 via shuttle or binding proteins (as NOS1AP) seems to be an important functional mechanism for NO synthases that produce short lived molecules like NO.

4.3. Currently known Studies on cardiac Function of Nos1ap and new Insights

We observed a significant reduction in the survival rate (60 % after 12 weeks vs. 100 % in non-induced mice) due to cardiac Nos1ap overexpression, therefore we could not confirm the published (Sugiyama et al., 2016) positive cardioprotective effect of Nos1ap. Sugiyama and colleagues (2016) found increased mortality in Nos1ap deleted mice but only as a consequence of oxidative stress. Opposite studies revealed upregulation of Nos1ap in MDX mice. MDX mice harboring a mutation in the dystrophin gene leads to muscular dystrophies also in the heart. The same group found overall lower S-nitrosylation of proteins and a reduced amplitude of calcium transients in cell culture experiments with neonatal rat cardiomyocytes in which Nos1ap expression was knocked down to ~30 % compared to wildtype cardiomyocytes. Moreover, they found the same co-localization of Nos1ap and the LTCC as we did (Section 1.5.) and suggested a role of Nos1ap on ion channel currents affecting action potential duration. (Treuer & Gonzalez, 2014). It is moreover possible, that Nos1ap acts as a regulator protein to compensate several cardiac diseases like arrhythmia or as a consequence of oxidative stress.

To our knowledge only one study examined the cardiac function in a transgenic mouse strain with a genetic deletion of Nos1ap. The authors focused on the effects of oxidative stress on Nos1ap deleted mice. Under basal conditions, as observed in our studies, there was no effect of the amount of Nos1ap on the expression of Nos subtypes on a cellular level. Also, they did not find any alterations in QRS or QT duration on ECG measurements due to deletion of Nos1ap and concluded that Nos1ap does not affect cardiac function under baseline conditions. However, induction of oxidative stress in Nos1ap knockout mice resulted in a higher mortality

with spontaneous ventricular tachyarrhythmias and a prolongation of APD_{90} in isolated cardiomyocytes. Interestingly, even under baseline conditions the Nos1ap knockout led to prolongation of APD_{90} in whole-cell patch-clamp measurements (Sugiyama et al., 2016). One of several identified SNPs in *NOS1AP* that is reported to modulate QT interval duration was analyzed in preliminary investigations (Section 1.5.). The mentioned SNP rs16847548 is associated with LQTS (Tomas et al., 2010; Arking et al., 2006; Crotti et al., 2009) and revealed a decreased transcriptional activity in a luciferase assay providing an explanation for the prolongation of APD_{90} due to Nos1ap deletion in mice. In line, our results showed a decrease of APD_{90} in Nos1ap overexpressing mice.

In another comprehensive study Ronchi at al. followed the idea, that Nos1ap polymorphisms cause Nos1 dysfunction and lead to an increased risk of cardiac arrhythmias. In guinea pig cardiomyocytes they found only a marginal affection of outward repolarizing currents (I_{Kr} and I_{Ks}) by Nos1 inhibition (Ronchi et al., 2021) but Nos1 inhibition significantly prolonged APD_{90}, supporting our assumption that there must be additional mechanisms for QT interval variations. Indeed, Ronchi and coworkers observed altered activities of inward LTCC currents during the plateau phase of membrane repolarization. They found downregulation of Nos1ap in combination with downregulation of Nos1 in human-induced pluripotent stem cell-cardiomyocytes (hiPSC-CMs) of a symptomatic LQT1 phenotype donor (with a mutation in *KCNQ1*) including two SNPs of NOS1AP (minor alleles). Furthermore, they obtained in the same hiPSC-CMs with the two minor Nos1ap alleles a prolonged APD_{90} and a larger peak $Ca_V1.2$ density in patch-clamp experiments compared with an asymptomatic LQT1 phenotype harboring the NOS1AP wildtype (major) allele. Since they confirmed the same results in hiPSC-CMs obtained from two healthy donors with minor and major NOS1AP allele, respectively, independence of Nos1ap-mediated pathways from the LQT1 phenotype was suspected (Ronchi et al., 2021). In comparing these results to our findings, we could confirm large parts of it. They also observed an interaction of Nos1ap with Nos1 and found downregulation of Nos1ap in donors with the minor alleles, similar as we found in promoter studies in our previous data. Downregulation of Nos1ap leads to prolongation of the QT interval, consistent with our findings of a shortening of the QT interval in Nos1ap overexpressing animals. However, the missing point in the Ronchi study was the investigation of interaction of LTCC with Nos1ap, as t-tubules are missing in hiPSC-CMs. In conclusion Nos1ap appears to act as an arrhythmogenic cofactor with impact on tethering Nos1 to target proteins.

Earle et al. points out in a hypertrophic cardiomyopathy registry-based study (n = 296) once more that two SNPs (rs10494366 and rs12143842) in the *NOS1AP* gene were linked to QTc interval prolongation (n = 228) without a higher risk of SCD in these patients (Earle et al., 2015). Finally, in a recent 2018 publication, Schwartz and colleagues examined the function of genetic modifiers, as the same disease-causing mutation can lead to different phenotypes and gradations of cardiac arrhythmias. “Modifier genes may promote higher risk for symptomatic disease and/or more severe disease expression, or might protect an individual from developing the disease” (Schwartz et al., 2018). In this study already five detrimental SNPs of Nos1ap were described as modifiers for QT interval prolonging effects or cardiac events.

As Nos1ap is described above as a modifier gene for QT interval variations, our results suggest more specifically a modulator function on the LTCC open probability affecting predisposition to arrhythmia susceptibility.

4.4. Impact of medical Compounds on Patients with genetic Variations in the *NOS1AP* Gene

As it seems evident, that NOS1AP SNPs have an effect on QT intervals, recent research focused on the response in QT duration in patients carrying genetic variations in the *NOS1AP* gene after drug administration. In mice with a Nos1ap deletion, administration of doxorubicin (25 mg/kg) led to longer QT intervals in the ECG and increased mortality (Sugiyama et al., 2016). Possibly Nos1ap could protect cardiac myocytes from oxidative stress and in the situation of a genetic deletion a mechanism for compensation of the oxidative stress might be missing, which then leads to fatal events in mice. It was speculated that Nos1ap-dependent guiding and tethering of Nos1 to subcellular targets is more relevant than the mere concentration of intracellular Nos1 levels. In line and as mentioned above, Burkard et al. (2010) found that translocation of Nos1 to mitochondria after ischemia, for example, protects against cell death by reducing ROS production in the mitochondria.

A large trial investigated the drug digoxin with regard on the impact of a *NOS1AP* gene variant and the correlating QT interval variations. Digoxin is given to patients with chronic atrial fibrillation or with HF and inhibits the sodium-potassium ATPase. A total of 10,057 participants were included in this trial and finally 249 participants obtained ECG recording during the digoxin therapy compared to 9,808 participants without digoxin therapy as control group. Interestingly the minor allele of *NOS1AP,* leading to prolongation of the QT interval, enhanced the effect of

digoxin significantly and resulted in a shorter mean QT interval duration (-23.9 ms) compared to participants carrying the major allele of *NOS1AP*. Soroush and her team explained that digoxin finally leads to increased intracellular calcium concentrations affecting ventricular repolarization (Soroush et al., 2022). Furthermore, minor alleles of *NOS1AP* result in higher sensitivity of QT prolonging effect of the calcium channel blocker verapamil (van Noord et al., 2009) as well of amiodarone (Jamshidi et al., 2012) indicating an impact of NOS1AP on drug effects on QT interval variations. Obviously, a physiological concentration of Nos1ap is important to balance calcium ion currents for a regular repolarization activity in cardiomyocytes. As the QT interval prolonging SNP rs16847548 in *NOS1AP* led to a reduced transcription rate (Section 1.5.) and our transgenic mouse model with a cardiac overexpression of Nos1ap revealed a shortening of the QT interval, we were able to prove that the imbalance of the Nos1ap level had a detrimental effect of cardiac electrophysiology with lethal consequences.

In agreement with Chang et al. (2013) NOS1AP is proposed as a new genetic marker for QT interval prolongation and SCD. Genetic variants of NOS1AP increase the risk of drug-induced prolongation of the QT interval (Chang et al., 2013). Another study analyzed the relation between different SNPs in *NOS1AP* and other genes previously associated with drug-induced QTc interval variations in the ECG and the QTc length in patients on methadone therapy at least three months after drug abuse. They found two *NOS1AP* SNPs which could be associated with QTc length but only one SNP in the potassium voltage-gated channel gene *KCNE1* remained significant after a statistical Bonferroni's correction. As a limitation of this study, 22.1 % of the subjects were under antipsychotic treatment known to prolong the QT interval. Furthermore, the ECG has not been measured prospectively in this patients and other risk factors associated with QT prolongation (e.g. potassium and magnesium serum concentrations) were not determined (Zerdazi et al., 2019). With these limitations and the fact that methadone blocks the hERG channel the results must be interpreted carefully.

In conclusion, we propose that Nos1ap modulates target proteins by affecting subcellular localization of Nos1 with subsequent local production of NO leading to posttranslational modification of target proteins (i.e., S-nitrosylation). In detail we found that the translocation of Nos1 to the LTCC led to an inhibition of calcium influx due to enhanced S-nitrosylation of LTCCs. In summary Nos1ap has an impact on the QT interval duration due to its modulator function on the LTCC open probability.

5. References

Aarnoudse, A. J., Newton-Cheh, C., de Bakker, P. I., Straus, S. M., Kors, J. A., Hofman, A., . . . Stricker, B. H. (2007). Common NOS1AP variants are associated with a prolonged QTc interval in the Rotterdam Study. *Circulation, 116*(1), 10-16. doi:10.1161/CIRCULATIONAHA.106.676783

Alonso, D., & Radomski, M. W. (2003). Nitric oxide, platelet function, myocardial infarction and reperfusion therapies. *Heart Fail Rev, 8*(1), 47-54. doi:10.1023/a:1022194921040

Amin, A. S., Tan, H. L., & Wilde, A. A. (2010). Cardiac ion channels in health and disease. *Heart Rhythm, 7*(1), 117-126. doi:10.1016/j.hrthm.2009.08.005

Arking, D. E., Pfeufer, A., Post, W., Kao, W. H., Newton-Cheh, C., Ikeda, M., . . . Chakravarti, A. (2006). A common genetic variant in the NOS1 regulator NOS1AP modulates cardiac repolarization. *Nat Genet, 38*(6), 644-651. doi:10.1038/ng1790

Arnold, W. P., Mittal, C. K., Katsuki, S., & Murad, F. (1977). Nitric oxide activates guanylate cyclase and increases guanosine 3':5'-cyclic monophosphate levels in various tissue preparations. *Proc Natl Acad Sci U S A, 74*(8), 3203-3207. doi:10.1073/pnas.74.8.3203

Beigi, F., Oskouei, B. N., Zheng, M., Cooke, C. A., Lamirault, G., & Hare, J. M. (2009). Cardiac nitric oxide synthase-1 localization within the cardiomyocyte is accompanied by the adaptor protein, CAPON. *Nitric Oxide, 21*(3-4), 226-233. doi:10.1016/j.niox.2009.09.005

Berger, S. M., & Bartsch, D. (2014). The role of L-type voltage-gated calcium channels Cav1.2 and Cav1.3 in normal and pathological brain function. *Cell Tissue Res, 357*(2), 463-476. doi:10.1007/s00441-014-1936-3

Bezzina, C. R., Lahrouchi, N., & Priori, S. G. (2015). Genetics of sudden cardiac death. *Circ Res, 116*(12), 1919-1936. doi:10.1161/CIRCRESAHA.116.304030

Blackwell, D. J., Schmeckpeper, J., & Knollmann, B. C. (2022). Animal Models to Study Cardiac Arrhythmias. *Circ Res, 130*(12), 1926-1964. doi:10.1161/CIRCRESAHA.122.320258

Bock, F. J., & Tait, S. W. G. (2020). Mitochondria as multifaceted regulators of cell death. *Nat Rev Mol Cell Biol, 21*(2), 85-100. doi:10.1038/s41580-019-0173-8

Bradford, M. M. (1976). A rapid and sensitive method for the quantitation of microgram quantities of protein utilizing the principle of protein-dye binding. *Anal Biochem, 72*, 248-254. doi:10.1006/abio.1976.9999

Bryan, N. S., Bian, K., & Murad, F. (2009). Discovery of the nitric oxide signaling pathway and targets for drug development. *Front Biosci (Landmark Ed), 14*, 1-18. doi:10.2741/3228

References

Burkard, N., Rokita, A. G., Kaufmann, S. G., Hallhuber, M., Wu, R., Hu, K., . . . Ritter, O. (2007). Conditional neuronal nitric oxide synthase overexpression impairs myocardial contractility. *Circ Res, 100*(3), e32-44. doi:10.1161/01.RES.0000259042.04576.6a

Burkard, N., Williams, T., Czolbe, M., Blomer, N., Panther, F., Link, M., . . . Ritter, O. (2010). Conditional overexpression of neuronal nitric oxide synthase is cardioprotective in ischemia/reperfusion. *Circulation, 122*(16), 1588-1603. doi:10.1161/CIRCULATIONAHA.109.933630

Campbell, M. G., Smith, B. C., Potter, C. S., Carragher, B., Marletta, M. A. (2014). Molecular architecture of mammalian nitric oxide synthases. *Proc Natl Acad Sci U S A,* 111(35), 3614-23. doi: 10.1073/pnas.1413763111

Chang, K. C., Barth, A. S., Sasano, T., Kizana, E., Kashiwakura, Y., Zhang, Y., . . . Marban, E. (2008). CAPON modulates cardiac repolarization via neuronal nitric oxide synthase signaling in the heart. *Proc Natl Acad Sci U S A, 105*(11), 4477-4482. doi:10.1073/pnas.0709118105

Chang, K. C., Sasano, T., Wang, Y. C., & Huang, S. K. (2013). Nitric Oxide Synthase 1 Adaptor Protein, an Emerging New Genetic Marker for QT Prolongation and Sudden Cardiac Death. *Acta Cardiol Sin, 29*(3), 217-225.

Crotti, L., Monti, M. C., Insolia, R., Peljto, A., Goosen, A., Brink, P. A., . . . George, A. L., Jr. (2009). NOS1AP is a genetic modifier of the long-QT syndrome. *Circulation, 120*(17), 1657-1663. doi:10.1161/CIRCULATIONAHA.109.879643

Dewenter, M., von der Lieth, A., Katus, H. A., & Backs, J. (2017). Calcium Signaling and Transcriptional Regulation in Cardiomyocytes. *Circ Res, 121*(8), 1000-1020. doi:10.1161/CIRCRESAHA.117.310355

Dronavalli, V. B., Ranasinghe, A. M., Venkateswaran, R. J., James, S. R., McCabe, C. J., Wilson, I. C., . . . Bonser, R. S. (2010). N-terminal pro-brain-type natriuretic peptide: a biochemical surrogate of cardiac function in the potential heart donor. *Eur J Cardiothorac Surg, 38*(2), 181-186. doi:10.1016/j.ejcts.2010.01.024

Earle, N., Ingles, J., Bagnall, R. D., Gray, B., Crawford, J., Smith, W., . . . Skinner, J. R. (2015). NOS1AP Polymorphisms Modify QTc Interval Duration But Not Cardiac Arrest Risk in Hypertrophic Cardiomyopathy. *J Cardiovasc Electrophysiol, 26*(12), 1346-1351. doi:10.1111/jce.12827

Fabiato, A., & Fabiato, F. (1979). Use of chlorotetracycline fluorescence to demonstrate Ca2+-induced release of Ca2+ from the sarcoplasmic reticulum of skinned cardiac cells. *Nature, 281*(5727), 146-148. doi:10.1038/281146a0

Garcia-Elias, A., & Benito, B. (2018). Ion Channel Disorders and Sudden Cardiac Death. *Int J Mol Sci, 19*(3). doi:10.3390/ijms19030692

Goldenberg, I., Moss, A. J., & Zareba, W. (2005). Sudden cardiac death without structural heart disease: update on the long QT and Brugada syndromes. *Curr Cardiol Rep, 7*(5), 349-356. doi:10.1007/s11886-005-0088-1

Gonzalez, D. R., Treuer, A., Sun, Q. A., Stamler, J. S., & Hare, J. M. (2009). S-Nitrosylation of cardiac ion channels. *J Cardiovasc Pharmacol, 54*(3), 188-195. doi:10.1097/FJC.0b013e3181b72c9f

Gordon, A. M., Homsher, E., & Regnier, M. (2000). Regulation of contraction in striated muscle. *Physiol Rev, 80*(2), 853-924. doi:10.1152/physrev.2000.80.2.853

Gordon, J. W., Scangos, G. A., Plotkin, D. J., Barbosa, J. A., & Ruddle, F. H. (1980). Genetic transformation of mouse embryos by microinjection of purified DNA. *Proc Natl Acad Sci U S A, 77*(12), 7380-7384. doi:10.1073/pnas.77.12.7380

Gossen, M., & Bujard, H. (1992). Tight control of gene expression in mammalian cells by tetracycline-responsive promoters. *Proc Natl Acad Sci U S A, 89*(12), 5547-5551. doi:10.1073/pnas.89.12.5547

Grilo, L. S., Carrupt, P. A., & Abriel, H. (2010). Stereoselective Inhibition of the hERG1 Potassium Channel. *Front Pharmacol, 1*, 137. doi:10.3389/fphar.2010.00137

Guo, T., Zhang, T., Mestril, R., & Bers, D. M. (2006). Ca2+/Calmodulin-dependent protein kinase II phosphorylation of ryanodine receptor does affect calcium sparks in mouse ventricular myocytes. *Circ Res, 99*(4), 398-406. doi:10.1161/01.RES.0000236756.06252.13

Hermosilla, T., Encina, M., Morales, D., Moreno, C., Conejeros, C., Alfaro-Valdes, H. M., . . . Varela, D. (2017). Prolonged AT1R activation induces CaV1.2 channel internalization in rat cardiomyocytes. *Sci Rep, 7*(1), 10131. doi:10.1038/s41598-017-10474-z

Hofmann, F., Lacinova, L., & Klugbauer, N. (1999). Voltage-dependent calcium channels: from structure to function. *Rev Physiol Biochem Pharmacol, 139*, 33-87.

Jaffrey, S. R., Benfenati, F., Snowman, A. M., Czernik, A. J., & Snyder, S. H. (2002). Neuronal nitric-oxide synthase localization mediated by a ternary complex with synapsin and CAPON. *Proc Natl Acad Sci U S A, 99*(5), 3199-3204. doi:10.1073/pnas.261705799

Jaffrey, S. R., Erdjument-Bromage, H., Ferris, C. D., Tempst, P., & Snyder, S. H. (2001). Protein S-nitrosylation: a physiological signal for neuronal nitric oxide. *Nat Cell Biol, 3*(2), 193-197. doi:10.1038/35055104

Jaffrey, S. R., Snowman, A. M., Eliasson, M. J., Cohen, N. A., & Snyder, S. H. (1998). CAPON: a protein associated with neuronal nitric oxide synthase that regulates its interactions with PSD95. *Neuron, 20*(1), 115-124. doi:10.1016/s0896-6273(00)80439-0

Jamshidi, Y., Nolte, I. M., Dalageorgou, C., Zheng, D., Johnson, T., Bastiaenen, R., . . . Behr, E. R. (2012). Common variation in the NOS1AP gene is associated with drug-induced QT prolongation and ventricular arrhythmia. *J Am Coll Cardiol, 60*(9), 841-850. doi:10.1016/j.jacc.2012.03.031

Kang, J., Wang, L., Chen, X. L., Triggle, D. J., & Rampe, D. (2001). Interactions of a series of fluoroquinolone antibacterial drugs with the human cardiac K+ channel HERG. *Mol Pharmacol, 59*(1), 122-126. doi:10.1124/mol.59.1.122

Kolder, I., Tanck, M. W. T., Postema, P. G., Barc, J., Sinner, M. F., Zumhagen, S., . . . Bezzina, C. R. (2015). Analysis for Genetic Modifiers of Disease Severity in Patients With Long-QT Syndrome Type 2. *Circ Cardiovasc Genet, 8*(3), 447-456. doi:10.1161/CIRCGENETICS.114.000785

Kunstyr, I., & Nicklas, W. (2000). *Rat pathogens: Control of SPF conditions, FELASA standards. In: The Laboratory Rat. Handbook of Experimental Animals Series.*: Academic Press, Chapter 8, 133-142, ISBN: 978-0-12-426400-7.

Lewalter, T., & Lüderitz, B. (2010). *Herzrhythmusstörungen*: Springer Medizin Verlag Heidelberg, ISBN: 978-3-540-76754-1.

Li, M. X., & Hwang, P. M. (2015). Structure and function of cardiac troponin C (TNNC1): Implications for heart failure, cardiomyopathies, and troponin modulating drugs. *Gene, 571*(2), 153-166. doi:10.1016/j.gene.2015.07.074

Loyer, X., Gomez, A. M., Milliez, P., Fernandez-Velasco, M., Vangheluwe, P., Vinet, L., . . . Heymes, C. (2008). Cardiomyocyte overexpression of neuronal nitric oxide synthase delays transition toward heart failure in response to pressure overload by preserving

calcium cycling. *Circulation, 117*(25), 3187-3198. doi:10.1161/CIRCULATIONAHA.107.741702

Martens, E., Sinner, M. F., Siebermair, J., Raufhake, C., Beckmann, B. M., Veith, S., . . . Kaab, S. (2014). Incidence of sudden cardiac death in Germany: results from an emergency medical service registry in Lower Saxony. *Europace, 16*(12), 1752-1758. doi:10.1093/europace/euu153

Mazzanti, A., Kanthan, A., Monteforte, N., Memmi, M., Bloise, R., Novelli, V., . . . Priori, S. G. (2014). Novel insight into the natural history of short QT syndrome. *J Am Coll Cardiol, 63*(13), 1300-1308. doi:10.1016/j.jacc.2013.09.078

Moon, A. L., Haan, N., Wilkinson, L. S., Thomas, K. L., & Hall, J. (2018). CACNA1C: Association With Psychiatric Disorders, Behavior, and Neurogenesis. *Schizophr Bull, 44*(5), 958-965. doi:10.1093/schbul/sby096

Mu, K., Sun, Y., Zhao, Y., Zhao, T., Li, Q., Zhang, M., . . . Jia, W. (2019). Hepatic nitric oxide synthase 1 adaptor protein regulates glucose homeostasis and hepatic insulin sensitivity in obese mice depending on its PDZ binding domain. *EBioMedicine, 47*, 352-364. doi:10.1016/j.ebiom.2019.08.033

Muruganandam, A., & Mutus, B. (1994). Isolation of nitric oxide synthase from human platelets. *Biochim Biophys Acta, 1200*(1), 1-6. doi:10.1016/0304-4165(94)90019-1

Ng, W. A., Grupp, I. L., Subramaniam, A., & Robbins, J. (1991). Cardiac myosin heavy chain mRNA expression and myocardial function in the mouse heart. *Circ Res, 68*(6), 1742-1750. doi:10.1161/01.res.68.6.1742

Numberger, M., & Draghuhn, A. (1996). *Patch-Clamp-Technik*: Spektrum Akademischer Verlag, ISBN: 9783827400239.

Ohno, S., Ozawa, J., Fukuyama, M., Makiyama, T., & Horie, M. (2020). An NGS-based genotyping in LQTS; minor genes are no longer minor. *J Hum Genet, 65*(12), 1083-1091. doi:10.1038/s10038-020-0805-z

Pang, L., Koren, G., Wang, Z., & Nattel, S. (2003). Tissue-specific expression of two human Ca(v)1.2 isoforms under the control of distinct 5' flanking regulatory elements. *FEBS Lett, 546*(2-3), 349-354. doi:10.1016/s0014-5793(03)00629-x

Priest, B. T., Bell, I. M., & Garcia, M. L. (2008). Role of hERG potassium channel assays in drug development. *Channels (Austin), 2*(2), 87-93. doi:10.4161/chan.2.2.6004

Reiser, P. J., Portman, M. A., Ning, X. H., & Schomisch Moravec, C. (2001). Human cardiac myosin heavy chain isoforms in fetal and failing adult atria and ventricles. *Am J Physiol Heart Circ Physiol, 280*(4), H1814-1820. doi:10.1152/ajpheart.2001.280.4.H1814

Ronchi, C., Bernardi, J., Mura, M., Stefanello, M., Badone, B., Rocchetti, M., . . . Zaza, A. (2021). NOS1AP polymorphisms reduce NOS1 activity and interact with prolonged repolarization in arrhythmogenesis. *Cardiovasc Res, 117*(2), 472-483. doi:10.1093/cvr/cvaa036

Roof, S. R., Ho, H. T., Little, S. C., Ostler, J. E., Brundage, E. A., Periasamy, M., . . . Ziolo, M. T. (2015). Obligatory role of neuronal nitric oxide synthase in the heart's antioxidant adaptation with exercise. *J Mol Cell Cardiol, 81*, 54-61. doi:10.1016/j.yjmcc.2015.01.003

Roussel, J., Champeroux, P., Roy, J., Richard, S., Fauconnier, J., Le Guennec, J. Y., & Thireau, J. (2016). The Complex QT/RR Relationship in Mice. *Sci Rep, 6*, 25388. doi:10.1038/srep25388

Sakmann, B., & Neher, E. (2009). *Single-Channel Recording*: Springer New York Dordrecht Heidelberg London, ISBN: 9781441912305.

Schuh, K., Uldrijan, S., Telkamp, M., Rothlein, N., & Neyses, L. (2001). The plasmamembrane calmodulin-dependent calcium pump: a major regulator of nitric oxide synthase I. *J Cell Biol, 155*(2), 201-205. doi:10.1083/jcb.200104131

Schwartz, P. J., Crotti, L., & George, A. L., Jr. (2018). Modifier genes for sudden cardiac death. *Eur Heart J, 39*(44), 3925-3931. doi:10.1093/eurheartj/ehy502

Schwartz, P. J., & Woosley, R. L. (2016). Predicting the Unpredictable: Drug-Induced QT Prolongation and Torsades de Pointes. *J Am Coll Cardiol, 67*(13), 1639-1650. doi:10.1016/j.jacc.2015.12.063

Sears, C. E., Ashley, E. A., & Casadei, B. (2004). Nitric oxide control of cardiac function: is neuronal nitric oxide synthase a key component? *Philos Trans R Soc Lond B Biol Sci, 359*(1446), 1021-1044. doi:10.1098/rstb.2004.1477

Shiels, H. A., & Galli, G. L. (2014). The sarcoplasmic reticulum and the evolution of the vertebrate heart. *Physiology (Bethesda), 29*(6), 456-469. doi:10.1152/physiol.00015.2014

Soroush, N., Aarnoudse, A. J., Kavousi, M., Kors, J. A., Ikram, M. A., Newton-Cheh, C., . . . Stricker, B. H. (2022). A NOS1AP gene variant is associated with a paradoxical increase of the QT-

interval shortening effect of digoxin. *Pharmacogenomics J, 22*(1), 55-61. doi:10.1038/s41397-021-00256-2

Spiranec, K., Chen, W., Werner, F., Nikolaev, V. O., Naruke, T., Koch, F., . . . Kuhn, M. (2018). Endothelial C-Type Natriuretic Peptide Acts on Pericytes to Regulate Microcirculatory Flow and Blood Pressure. *Circulation, 138*(5), 494-508. doi:10.1161/CIRCULATIONAHA.117.033383

Stamler, J. S., Toone, E. J., Lipton, S. A., & Sucher, N. J. (1997). (S)NO signals: translocation, regulation, and a consensus motif. *Neuron, 18*(5), 691-696. doi:10.1016/s0896-6273(00)80310-4

Strasen, J., & Ritter, O. (2011). Role of nNOS in cardiac ischemia-reperfusion injury. *Trends Cardiovasc Med, 21*(2), 58-63. doi:10.1016/j.tcm.2012.03.001

Strobach, D., Schlattl, A., Schiek, S., & Bertsche, T. (2021). QTc-time-prolongating drugs and additional risk factors for long-QT-syndrome at hospital admission of surgical patients - risk assessment by pharmacists. *Pharmazie, 76*(11), 562-566. doi:10.1691/ph.2021.1697

Suessbrich, H., Schonherr, R., Heinemann, S. H., Attali, B., Lang, F., & Busch, A. E. (1997). The inhibitory effect of the antipsychotic drug haloperidol on HERG potassium channels expressed in Xenopus oocytes. *Br J Pharmacol, 120*(5), 968-974. doi:10.1038/sj.bjp.0700989

Sugiyama, K., Sasano, T., Kurokawa, J., Takahashi, K., Okamura, T., Kato, N., . . . Furukawa, T. (2016). Oxidative Stress Induced Ventricular Arrhythmia and Impairment of Cardiac Function in Nos1ap Deleted Mice. *Int Heart J, 57*(3), 341-349. doi:10.1536/ihj.15-471

Sun, J., Picht, E., Ginsburg, K. S., Bers, D. M., Steenbergen, C., & Murphy, E. (2006). Hypercontractile female hearts exhibit increased S-nitrosylation of the L-type Ca2+ channel alpha1 subunit and reduced ischemia/reperfusion injury. *Circ Res, 98*(3), 403-411. doi:10.1161/01.RES.0000202707.79018.0a

Tang, W., Kang, J., Wu, X., Rampe, D., Wang, L., Shen, H., . . . Garyantes, T. (2001). Development and evaluation of high throughput functional assay methods for HERG potassium channel. *J Biomol Screen, 6*(5), 325-331. doi:10.1177/108705710100600506

Tester, D. J., & Ackerman, M. J. (2014). Genetics of long QT syndrome. *Methodist Debakey Cardiovasc J, 10*(1), 29-33. doi:10.14797/mdcj-10-1-29

Tomas, M., Napolitano, C., De Giuli, L., Bloise, R., Subirana, I., Malovini, A., . . . Priori, S. G. (2010). Polymorphisms in the NOS1AP gene modulate QT interval duration and risk of arrhythmias in the long QT syndrome. *J Am Coll Cardiol, 55*(24), 2745-2752. doi:10.1016/j.jacc.2009.12.065

Treuer, A. V., & Gonzalez, D. R. (2014). NOS1AP modulates intracellular Ca(2+) in cardiac myocytes and is up-regulated in dystrophic cardiomyopathy. *Int J Physiol Pathophysiol Pharmacol, 6*(1), 37-46.

van Noord, C., Aarnoudse, A. J., Eijgelsheim, M., Sturkenboom, M. C., Straus, S. M., Hofman, A., . . . Stricker, B. H. (2009). Calcium channel blockers, NOS1AP, and heart-rate-corrected QT prolongation. *Pharmacogenet Genomics, 19*(4), 260-266. doi:10.1097/FPC.0b013e328324e556

Yang, D., Zhu, W. Z., Xiao, B., Brochet, D. X., Chen, S. R., Lakatta, E. G., . . . Cheng, H. (2007). Ca2+/calmodulin kinase II-dependent phosphorylation of ryanodine receptors suppresses Ca2+ sparks and Ca2+ waves in cardiac myocytes. *Circ Res, 100*(3), 399-407. doi:10.1161/01.RES.0000258022.13090.55

Yin, F. C., Spurgeon, H. A., Rakusan, K., Weisfeldt, M. L., & Lakatta, E. G. (1982). Use of tibial length to quantify cardiac hypertrophy: application in the aging rat. *Am J Physiol, 243*(6), H941-947. doi:10.1152/ajpheart.1982.243.6.H941

Zang, X., Li, S., Zhao, Y., Chen, K., Wang, X., Song, W., . . . Gao, C. (2019). Systematic Meta-Analysis of the Association Between a Common NOS1AP Genetic Polymorphism, the QTc Interval, and Sudden Death. *Int Heart J, 60*(5), 1083-1090. doi:10.1536/ihj.19-024

Zareba, W., Moss, A. J., le Cessie, S., Locati, E. H., Robinson, J. L., Hall, W. J., & Andrews, M. L. (1995). Risk of cardiac events in family members of patients with long QT syndrome. *J Am Coll Cardiol, 26*(7), 1685-1691. doi:10.1016/0735-1097(95)60383-2

Zerdazi, E. H., Vorspan, F., Marees, A. T., Naccache, F., Lepine, J. P., Laplanche, J. L., . . . Bloch, V. (2019). QT length during methadone maintenance treatment: gene x dose interaction. *Fundam Clin Pharmacol, 33*(1), 96-106. doi:10.1111/fcp.12405

Zhang, R., Chen, F., Yu, H., Gao, L., Yin, X., Dong, Y., . . . Xia, Y. (2017). The genetic variation rs12143842 in NOS1AP increases idiopathic ventricular tachycardia risk in Chinese Han populations. *Sci Rep, 7*(1), 8356. doi:10.1038/s41598-017-08548-z

Zheng, Y., Li, H., Qin, W., Chen, W., Duan, Y., Xiao, Y., . . . He, L. (2005). Association of the carboxyl-terminal PDZ ligand of neuronal nitric oxide synthase gene with schizophrenia

in the Chinese Han population. *Biochem Biophys Res Commun, 328*(4), 809-815. doi:10.1016/j.bbrc.2005.01.037

Zhou, M. H., Bavencoffe, A., & Pan, H. L. (2015). Molecular Basis of Regulating High Voltage-Activated Calcium Channels by S-Nitrosylation. *J Biol Chem, 290*(51), 30616-30623. doi:10.1074/jbc.M115.685206

6. List of Figures

7. List of Tables

8. List of Abbreviations

°C	degree Celsius
αMHC-tTA	tetracycline-controlled transactivator protein (tTA) under the regulatory control of the rat alpha myosin heavy chain promoter (αMHC)
ad libitum	diet is available at all times
Ampr	ampicillin resistance gene
AP	action potential
APD_{90}	action potential duration at 90 % of repolarization / Dauer des Aktionspotentials nach 90 % der Repolarisation
APS	ammonium persulfate
ATP	adenosine triphosphate
BSA	bovine serum albumin
BNP	brain natriuretic peptide
bp	base pair
CACNA1C	calcium voltage-gated channel subunit alpha1 C
$Ca_V1.2$	voltage-gated L-type calcium channel, exclusively the cardiac subtype
CaMKII	calcium/calmodulin-dependent kinase II
CaM	calcium-calmodulin
cAMP	cyclic adenosine monophosphate
Capon	carboxyl-terminal PDZ ligand of nitric oxide synthase 1 (alias for Nos1ap)
cDNA	complementary DNA
cGMP	cyclic guanosine monophosphate
DHPR	dihydropyridine receptor
dH2O	distilled water
DT	double transgenic
DTT	dithiothreitol
EC	excitation-contraction
ECG	electrocardiogram
et al.	*et alii* (and others)
FAD	flavin adenine dinucleotide
FMN	flavin mononucleotide
Gapdh	Glyceraldehyde-3-phosphate dehydrogenase

H&E	hematoxylin-eosin (for morphological staining)
hERG1	“human ether à-gogo related gene 1” = KCNH2
HF	heart failure
Hind III	restriction site for *Hind* III restriction enzyme isolated from *Haemophilus influenza*
hiPSC-CM	induced human pluripotent stem cell-derived cardiomyocyte
HRP	horseradish peroxidase
HVA	high-voltage-activated channels
$I_{Ca\text{-}L}$	slow calcium inward currents
I_{K1}	inwardly rectifying potassium current
I_{Kr}	rapid outward potassium currents
I_{Kr}	slow outward potassium currents
I_{Na}	fast sodium inward current
I_{to}	transient outward potassium currents
in vivo	inside a living body
in vitro	outside the body in artificial conditions
ICD	implantable cardioverter-defibrillator
K	potassium
KCl	potassium chloride
KCNQ1	potassium voltage-gated channel subfamily Q member 1
KCNH2	potassium voltage-gated channel subfamily H member 2
LQTS	*long* QT Syndrom / long QT syndrome
LTCC	L-type calcium channel (auch CaV1.2) / L-Typ Calciumkanal
MCS	multiple cloning site
MHC	myosin heavy chain
MTSEA	methanethiosulfonate ethylammonium
MI	myocardial infarction
NaCl	sodium chloride
NADPH	nicotinamide adenine dinucleotide phosphate
NCX	sodium/calcium exchanger
NO	nitric oxide
NOS1AP	neuronal nitric oxide synthase 1 (NOS1) adaptor protein (earlier: Capon)

List of Abbreviations

NT-proBNP	N-terminal pro-brain-type natriuretic peptide
ori	origin of replication
PCR	polymerase chain reaction
PKA/G	protein kinase A/G
PLN	phospholamban
PMCA	plasma membrane calcium ATPase
PMCA4b	a cardiac isoform 4b of PMCA
PMSF	phenylmethylsulfonyl fluoride
QTc	corrected QT interval duration according to the formula of Bazett
ROS	reactive oxygen species
RT	room temperature
RyR	ryanodine receptors
SCD	sudden cardiac death
SCN5A	sodium voltage-gated channel alpha subunit 5
SDS	sodium dodecyl sulfate
SEM	standard deviation
SERCA	SR calcium ATPase
SERCA2a	subtype 2a of SERCA expressed in heart
siRNA	RNA silencing
SNAP	S-nitroso-N-acetyl-DL-penicillamine
SNP	single nucleotide polymorphism
SPF	specific pathogen free
SQTS	*short* QT Syndrom / short QT syndrome
SR	sarcoplasmic reticulum
TAC	transverse aortic constriction
Taq	*Taq* DNA Polymerase of *Thermus aquaticus* without proof reading-function
1x TBST	1x Tris-Buffered Saline with 0.1 % Tween 20
TCF	transgenic core facility
Temed	tetramethylethylenediamine
TRE	tetracycline-responsive element
tTA	tetracycline-controlled transactivator protein
Xba I	restriction site for *Xba* I restriction enzyme isolated from *Xanthomonas badrii*

9. Appendix

A1: Protein sequence NOS1AP Isoform 1 (UniProt identifier: Q9D3A8-1, length: 503 amino acids, 55,87 kDa, 9-6-2022)

MPSKTKYNLVDDGHDLRIPLHNEDAFQHGISFEAKYVGSLDVPRPNSRVEIVAAMRRIRYEFKAKNIKKKKVSIMVSVD
GVKVILKKKKKKKEWTWDESKMLVMQDPIYRIFYVSHDSQDLKIFSYIARDGASNIFRCNVFKSKKKSQAMRIVRTVG
QAFEVCHKLSLQHTQQNADGQEDGESERNSDGSGDPGRQLTGAERVSTAAAEETDIDAVEVPLPGNDILEFSRGVT
DLDAVGKDGGSHIDSTVSPHPQEPMLTASPRMLLPSSSSKPPGLGTGTPLSTHHQMQLLQQLLQQQQQQTQVAVA
QVHLLKDQLAAEAAARLEAQARVHQLLLQNKDMLQHISLLVKQVQELELKLSGQNTMGSQDSLLEITFRSGALPVLC
ESTTPKPEDLHSPLLGAGLADFAHPAGSPLGRHDCLVKLECFRFLPPEDTQPMMAQGEPLLGGLELIKFRESGIASEYE
SNTDESEERDSWSQEELPRLLNVLQRQELGDSLDDEIAV

A2: Complete pTRE-6xHN-Nos1ap plasmid sequence. Find following markings of structural elements. ATG/TGA start/stop codon. 6x-HN affinity tag. *Hind* III & *Xba* I restriction sites. Nos1ap insert (length: 1.509 kb). NOS1AP3 & NOS1AP5 genotyping primer pair.

CTCGAGTTTACCACTCCCTATCAGTGATAGAGAAAAGTGAAAGTCGAGTTTACCACTCCCTATCAGTGATAGAGA
AAAGTGAAAGTCGAGTTTACCACTCCCTATCAGTGATAGAGAAAAGTGAAAGTCGAGTTTACCACTCCCTATCA
GTGATAGAGAAAAGTGAAAGTCGAGTTTACCACTCCCTATCAGTGATAGAGAAAAGTGAAAGTCGAGTTTACCA
CTCCCTATCAGTGATAGAGAAAAGTGAAAGTCGAGTTTACCACTCCCTATCAGTGATAGAGAAAAGTGAAAGTC
GAGCTCGGTACCCGGGTCGAGTAGGCGTGTACGGTGGGAGGCCTATATAAGCAGAGCTCGTTTAGTGAACCGT
CAGATCGCCTGGAGACGCCATCCACGCTGTTTTGACCTCCATAGAAGACACCGGGACCGATCCAGCCTCCGCGG
CCCCGAATTCGAGCTCGGTACCCGGGGATCCTCTAGTCAGCTGACGCGAGCTAGACACCATGAGACATAATCAT
AATCATAATCATAATCATAATCACAACCTTATGGCCATGGAGGCCCAAGCTTATGCCACCATGCCCAGCAAGACC
AAGTACAACCTGGTGGACGACGGCCACGACCTGCGGATCCCCCTGCACAACGAGGACGCCTTCCAGCACGGCA
TCAGCTTCGAGGCCAAATACGTGGGCAGCCTGGACGTGCCCAGACCCAACAGCCGGGTGGAAATCGTGGCCGC
CATGCGGCGGATCAGATACGAGTTCAAGGCCAAGAACATCAAGAAAAAGAAAGTGTCCATCATGGTGTCCGTG
GACGGCGTGAAAGTGATCCTGAAGAAGAAGAAAAAGAAAAAAGAGTGGACCTGGGACGAGAGCAAGATGCT
GGTCATGCAGGACCCCATCTACCGGATCTTCTACGTGTCCCACGACAGCCAGGACCTGAAGATTTTCAGCTATAT
CGCCCGGGACGGCGCCAGCAACATCTTCCGGTGCAACGTGTTCAAGAGCAAGAAAAAGTCCCAGGCCATGCGG
ATCGTGCGGACAGTGGGCCAGGCCTTCGAAGTGTGCCACAAGCTGAGCCTGCAGCACACCCAGCAGAACGCCG
ACGGCCAGGAAGATGGCGAGAGCGAGCGGAACAGCGACGGCTCTGGCGACCCTGGCAGACAGCTGACAGGC
GCCGAGAGAGTGTCCACCGCCGCTGCCGAGGAAACCGACATCGACGCCGTGGAAGTGCCCCTGCCCGGCAAC
GACATCCTGGAATTCAGCAGAGGCGTGACCGACCTGGATGCCGTGGGCAAGGATGGCGGCAGCCACATCGAC
AGCACCGTGTCCCCACACCCCCAAGAACCCATGCTGACCGCCAGCCCCAGAATGCTGCTGCCCAGCTCTAGCTC
CAAGCCTCCTGGCCTGGGCACCGGCACCCCTCTGTCTACCCACCACCAGATGCAGCTGCTGCAACAGCTCCTCC
AGCAGCAGCAGCAGCAGACCCAGGTGGCCGTGGCTCAGGTGCACCTCCTGAAGGATCAGCTGGCCGCCGAGG
CCGCTGCCAGACTGGAAGCTCAGGCCAGAGTGCACCAGCTGCTGCTCCAGAACAAGGACATGCTGCAGCACAT
CAGCCTGCTGGTCAAACAGGTGCAGGAACTGGAACTGAAGCTGAGCGGCCAGAACACCATGGGCAGCCAGGA
CTCCCTGCTGGAAATCACCTTCAGATCTGGCGCCCTGCCCGTGCTGTGTGAGAGCACCACCCCCAAGCCCGAGG
ACCTGCATAGCCCTCTGCTGGGAGCCGGCCTGGCCGATTTTGCCCATCCTGCTGGCAGCCCCCTGGGCAGACAC
GATTGCCTGGTCAAGCTGGAATGCTTCCGGTTCCTGCCCCCCGAGGACACCCAGCCTATGATGGCCCAGGGCG
AGCCACTGCTGGGCGGCCTGGAACTGATCAAGTTCAGAGAGAGCGGAATCGCCAGCGAGTACGAGAGCAACA
CCGACGAGAGCGAGGAACGGGACAGCTGGTCCCAGGAAGAACTGCCCCGGCTGCTGAACGTGCTGCAGAGAC
AGGAACTGGGCGACTCCCTGGACGACGAGATCGCCGTGTGATAATCTAGAGCTGAGAACTTCAGGGTGAGTTT
GGGGACCCTTGATTGTTCTTTCTTTTTCGCTATTGAAAAATTCATGTTATATGGAGGGGGCAAAGTTTTCAGGGT
GTTGTTTAGAATGGGAAGATGTCCCTTGTATCACCATGGACCCTCATGATAATTTTGTTTCTTTCACTTTCTACTCT
GTTGACAACCATTGTCTCCTCTTATTTTCTTTTCATTTTCTGTAACTTTTTTCGTTAAACTTTAGCTTGCATTTGTAA
CGAATTTTTAAATTCACTTTCGTTTATTTGTCAGATTGTAAGTACTTTCTCTAATCACTTTTTTTTCAAGGCAATCA

GGGTAATTATATTGTACTTCAGCACAGTTTTAGAGAACAATTGTTATAATTAAATGATAAGGTAGAATATTTCTG
CATATAAATTCTGGCTGGCGTGGAAATATTCTTATTGGTAGAAACAACTACATCCTGGTAATCATCCTGCCTTTCT
CTTTATGGTTACAATGATATACACTGTTTGAGATGAGGATAAAATACTCTGAGTCCAAACCGGGCCCCTCTGCTA
ACCATGTTCATGCCTTCTTCTTTTTCCTACAGCTCCTGGGCAACGTGCTGGTTGTTGTGCTGTCTCATCATTTTGG
CAAAGAATTCACTCCTCAGGTGCAGGCTGCCTATCAGAAGGTGGTGGCTGGTGTGGCCAATGCCCTGGCTCAC
AAATACCACTGAGATCTTTTTCCCTCTGCCAAAAATTATGGGGACATCATGAAGCCCCTTGAGCATCTGACTTCT
GGGTAATAAAGGAAATTTATTTTCATTGCAATAGTGTGTGGGAATTTTTTGTGTCTCTCACTCGGAAGGACATAT
GGGAGGGCAAATCATTTAAAACATCAGAATGAGTATTTGGTTTAGAGTTTGGCAACATATGCCATATGCTGGCT
GCCATGAACAAAGGTGGCTATAAAGAGGTCATCAGTATATGAAACAGCCCCCTGCTGTCCATTCCTTATTCCATA
GAAAAGCCTTGACTTGAGGTTAGATTTTTTTTATATTTTGTTTTGTGTTATTTTTTTCTTTAACATCCCTAAAATTTT
CCTTACATGTTTTACTGCCAGATTTTTCCTCCTCTCCTGACTACTCCCAGTCATAGCTGTCCCTCTTCTCTTATGAA
CTCGACTGCATTAATGAATCGGCCAACGCGCGGGGAGAGGCGGTTTGCGTATTGGGCGCTCTTCCGCTTCCTCG
CTCACTGACTCGCTGCGCTCGGTCGTTCGGCTGCGGCGAGCGGTATCAGCTCACTCAAAGGCGGTAATACGGTT
ATCCACAGAATCAGGGGATAACGCAGGAAAGAACATGTGAGCAAAAGGCCAGCAAAAGGCCAGGAACCGTAA
AAAGGCCGCGTTGCTGGCGTTTTTCCATAGGCTCCGCCCCCCTGACGAGCATCACAAAAATCGACGCTCAAGTC
AGAGGTGGCGAAACCCGACAGGACTATAAAGATACCAGGCGTTTCCCCCTGGAAGCTCCCTCGTGCGCTCTCCT
GTTCCGACCCTGCCGCTTACCGGATACCTGTCCGCCTTTCTCCCTTCGGGAAGCGTGGCGCTTTCTCAATGCTCA
CGCTGTAGGTATCTCAGTTCGGTGTAGGTCGTTCGCTCCAAGCTGGGCTGTGTGCACGAACCCCCCGTTCAGCC
CGACCGCTGCGCCTTATCCGGTAACTATCGTCTTGAGTCCAACCCGGTAAGACACGACTTATCGCCACTGGCAG
CAGCCACTGGTAACAGGATTAGCAGAGCGAGGTATGTAGGCGGTGCTACAGAGTTCTTGAAGTGGTGGCCTAA
CTACGGCTACACTAGAAGGACAGTATTTGGTATCTGCGCTCTGCTGAAGCCAGTTACCTTCGGAAAAAGAGTTG
GTAGCTCTTGATCCGGCAAACAAACCACCGCTGGTAGCGGTGGTTTTTTTGTTTGCAAGCAGCAGATTACGCGC
AGAAAAAAAGGATCTCAAGAAGATCCTTTGATCTTTTCTACGGGGTCTGACGCTCAGTGGAACGAAAACTCACG
TTAAGGGATTTTGGTCATGAGATTATCAAAAAGGATCTTCACCTAGATCCTTTTAAATTAAAAATGAAGTTTTAAA
TCAATCTAAAGTATATATGAGTAAACTTGGTCTGACAGTTACCAATGCTTAATCAGTGAGGCACCTATCTCAGCG
ATCTGTCTATTTCGTTCATCCATAGTTGCCTGACTCCCCGTCGTGTAGATAACTACGATACGGGAGGGCTTACCA
TCTGGCCCCAGTGCTGCAATGATACCGCGAGACCCACGCTCACCGGCTCCAGATTTATCAGCAATAAACCAGCC
AGCCGGAAGGGCCGAGCGCAGAAGTGGTCCTGCAACTTTATCCGCCTCCATCCAGTCTATTAATTGTTGCCGGG
AAGCTAGAGTAAGTAGTTCGCCAGTTAATAGTTTGCGCAACGTTGTTGCCATTGCTACGGCATCGTGGTGTCAC
GCTCGTCGTTTGGTATGGCTTCATTCAGCTCCGGTTCCCAACGATCAAGGCGAGTTACATGATCCCCCATGTTGT
GCAAAAAAGCGGTTAGCTCCTTCGGTCCTCCGATCGTTGTCAGAAGTAAGTTGGCCGCAGTGTTATCACTCATG
GTTATGGCAGCACTGCATAATTCTCTTACTGTCATGCCATCCGTAAGATGCTTTTCTGTGACTGGTGAGTACTCA
ACCAAGTCATTCTGAGAATAGTGTATGCGGCGACCGAGTTGCTCTTGCCCGGCGTCAATACGGGATAATACCGC
GCCACATAGCAGAACTTTAAAAGTGCTCATCATTGGAAAACGTTCTTCGGGGCGAAAACTCTCAAGGATCTTAC
CGCTGTTGAGATCCAGTTCGATGTAACCCACTCGTGCACCCAACTGATCTTCAGCATCTTTTACTTTCACCAGCGT
TTCTGGGTGAGCAAAAACAGGAAGGCAAAATGCCGCAAAAAAGGGAATAAGGGCGACACGGAAATGTTGAAT
ACTCATACTCTTCCTTTTTCAATATTATTGAAGCATTTATCAGGGTTATTGTCTCATGAGCGGATACATATTTGAAT
GTATTTAGAAAAATAAACAAATAGGGGTTCCGCGCACATTTCCCCGAAAAGTGCCACCTGACGTCTAAGAAACC
ATTATTATCATGACATTAACCTATAAAAATAGGCGTATCACGAGGCCCTTTCGT

10. Acknowledgement

11. Curriculum vitae

12. Declaration

Eidesstaatliche Versicherung

Ich versichere an Eides statt durch meine Unterschrift, dass ich die vorstehende Arbeit selbständig und ohne fremde Hilfe angefertigt und alle Stellen, die ich wörtlich oder annähernd wörtlich aus Veröffentlichungen entnommen habe, als solche kenntlich gemacht habe, mich auch keiner anderen als der angegebenen Literatur oder sonstiger Hilfsmittel bedient habe. Die Arbeit hat in dieser oder ähnlicher Form noch keiner anderen Prüfungsbehörde vorgelegen. Zudem erkläre ich mich damit einverstanden, dass meine Arbeit mit einer Plagiatssoftware geprüft wird.

Brandenburg an der Havel, September 2022 *Monique Heidrun Jänsch*